Quaternary Science Reviews 282 (2022) 107433

Contents lists available at ScienceDirect

Quaternary Science Reviews

journal homepage: www.elsevier.com/locate/quascirev

Late Plio-Pleistocene evolution of the Eurasian Ice Sheets inferred from sediment input along the northeastern Atlantic continental margin

Øyvind Flataker Lien [a, *], Berit O. Hjelstuen [a], Xu Zhang [b], Hans Petter Sejrup [a]

[a] Department of Earth Science, University of Bergen, Allégaten 41, N-5007, Bergen, Norway
[b] Group of Alpine Paleoecology and Human Adaptation (ALPHA), State Key Laboratory of Tibetan Plateau Earth System, Resources and Environment (TPESRE), Institute of Tibetan Plateau Research, Chinese Academy of Sciences, Beijing, 100101, China

ARTICLE INFO

Article history:
Received 28 October 2021
Received in revised form
14 February 2022
Accepted 18 February 2022
Available online 11 March 2022

Handling Editor: C. O'Cofaigh

Keywords:
Eurasian Ice Sheets
Late Plio-Pleistocene
Ice sheet development
Sediment volumes
Erosion rates
Sedimentation rates
Glacial dynamics

ABSTRACT

High-latitude marine sediment archives may contain information about the configuration and dynamics of former ice sheets, paleoclimate and the intensity of glacial erosion and uplift in catchment areas. Compiling information on the Late Cenozoic sediment packages along the NE Atlantic continental margin shows that large sediment volumes (c. 982 $\times$ 10^3 km^3) were deposited during the Northern Hemisphere Glaciations (NHG), and that significant spatial and temporal variations in sediment input occurred during three distinct NHG Phases. NHG Phase I (2.7–1.5 Ma) was characterized by high sediment input to the trough mouth fan systems offshore Svalbard, suggesting strong glacial erosion and the development of large ice sheets over Svalbard. Comparatively moderate sedimentation and erosion rates are observed along the SW Barents Sea and the Norwegian margins during NHG Phase I. This indicates more restricted ice sheets over Fennoscandia compared to Svalbard, although periods of shelf edge glaciation most likely occurred. The most prominent overall margin development occurred during NHG Phase II (1.5–0.8 Ma), when recurrent large-scale, continental shelf edge, glaciations are suggested for the entire Eurasian Ice Sheets (EurIS). Compared to NHG Phase I, average sedimentation rates are three (91 cm/kyr) and two times higher (20 cm/kyr), respectively, in the Kara-Barents Sea-Svalbard Ice Sheet (KBSIS) region and the Fennoscandian/British-Irish Ice Sheet (FIS/BIIS) region. During NHG Phase III (0.8–0 Ma), sediment input decreases considerably (73%) along the marine margin of the KBSIS, while increasing significantly (62%) from the FIS/BIIS, in comparison to NHG Phase II. These estimates mark a major transition in the evolution of the EurIS, where the submergence below sea level of the Barents Sea region and the initiation of the Norwegian Channel Ice Stream are suggested to be key factors in this change. Furthermore, the submergence of the Barents Sea region affected ocean-atmosphere coupling and circulation which may have had a potential impact on global long-term climate change.

1. Introduction

With the onset of the Late Plio-Pleistocene Northern Hemisphere Glaciations (NHG), there was a prominent shift in depositional patterns along the Northeastern (NE) Atlantic continental margin, as prograding wedges and trough mouth fans (TMFs) started to accumulate (Figs. 1 and 2) (e.g., Faleide et al., 1996; Vorren et al., 1998; Dahlgren et al., 2005; Nielsen et al., 2005; Anell et al., 2010). These changes in the depositional system have been linked with the development of the Fennoscandian (FIS), the Kara-Barents Sea-Svalbard (KBSIS), and the British-Irish (BIIS) ice sheets (Fig. 1A), which during some periods coalesced into the Eurasian Ice Sheets (EurIS) (e.g., Sejrup et al., 2005). The Late Cenozoic glacial succession along the NE Atlantic continental margin represents important marine archives as they enable studies of the development of the ice ages, long-term landscape evolution, onshore/offshore uplift and subsidence patterns, and the burial history of hydrocarbon reservoirs (e.g., Dowdeswell et al., 2010; Steer et al., 2012; Andersen et al., 2018; Fjeldskaar and Amantov, 2018; Lasabuda et al., 2021). Furthermore, such sediment archives have the potential to uncover the history of paleo-ice sheet dynamics

* Corresponding author.
E-mail address: oyvind.lien@uib.no (Ø.F. Lien).

https://doi.org/10.1016/j.quascirev.2022.107433

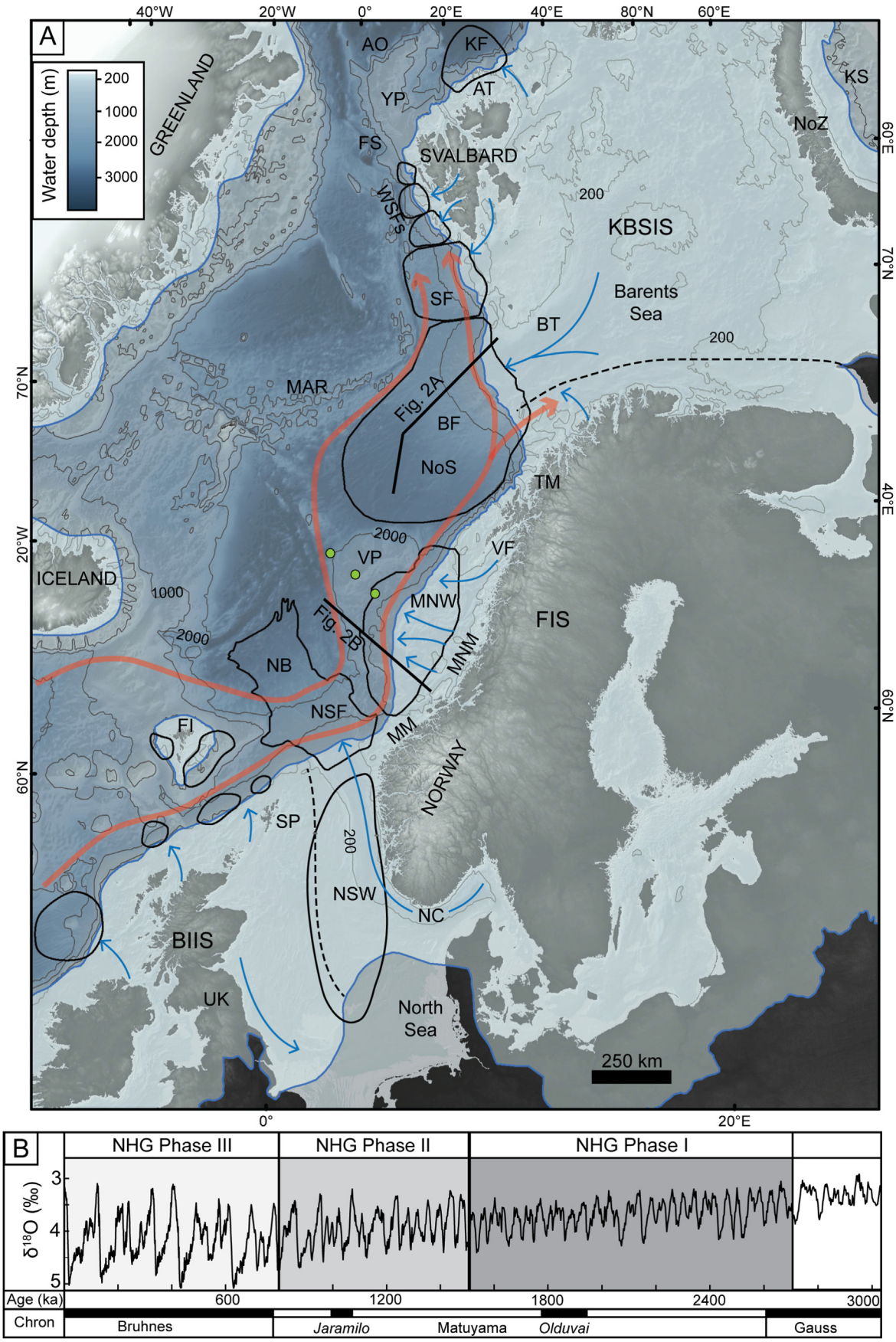
A
Water depth (m)
200
1000
2000
3000
GREENLAND
ICELAND
SVALBARD
AO
KF
AT
YP
FS
WSFs
KS
NoZ
KBSIS
Barents Sea
SF
BT
MAR
Fig. 2A
BF
NoS
TM
VP
VF
MNW
MNM
FIS
Fig. 2B
NB
NSF
FI
MM
NORWAY
SP
NSW
NC
BIIS
UK
North Sea
250 km
40°W
20°W
0°
20°E
40°E
80°N
60°E
70°N
60°N
B
NHG Phase III
NHG Phase II
NHG Phase I
δ18O (‰)
Age (ka)
600
1200
1800
2400
3000
Chron
Bruhnes
Jaramilo
Matuyama
Olduvai
Gauss

Fig. 1. (A) NE Atlantic continental margin with outline of TMFs and prograding wedges (black polygons) (based on Dahlgren et al., 2005). Warm surface water in the Norwegian Atlantic Current is indicated by red arrows (based on Orvik and Niiler, 2002). Major Late Weichselian ice streams (blue arrows) (based on Ottesen et al., 2005) and the ice extent during the Last Glacial Maximum (from Patton et al., 2017) are also shown (blue polygon). Green circles are ODP sites 642, 643 and 644. The stippled lines separate the different ice sheets from each other. Bathymetric and terrestrial data are from GEBCO's global ocean and land terrain models (http://www.gebco.net/). AO: Arctic Ocean, AT: Albertini Trough, BF: Bjørnøya TMF, BIIS: British-Irish Ice Sheet, BS: Barents Sea, BT: Bjørnøya Trough, BT: Bjørnøya Trough, FI: Faroe Islands, FIS: Fennoscandic Ice Sheet, FS: Fram Strait, KS: Kara Sea, KBSIS: Kara-Barents Sea-Svalbard Ice Sheet, KF: Kvitøya TMF, MM: Møre margin, MNM: Mid-Norwegian margin, MNW: Mid-Norwegian wedge, NB: Norway Basin, NC: Norwegian Channel, NoS: Nordic Seas, NoZ: Novaya Zemlya, NS: North Sea, NSF: North Sea TMF, NSW: North Sea wedge, SF: Storfjorden TMF, SP: Shetland Platform, ST: Storfjorden Trough, TM: Troms Margin, VF: Vestfjorden, VP: Vøring Plateau, WSFs: Western Svalbard TMFs, YP: Yermak Plateau. **(B)** $\delta^{18}O$ marine isotope curve for the last 3 Myr (from Lisiecki and Raymo, 2005) and geomagnetic polarity chrons. The three studied time periods in the EurIS development, NHG Phases I-III are also indicated. (For interpretation of the references to color in this figure legend, the reader is referred to the Web version of this article.)

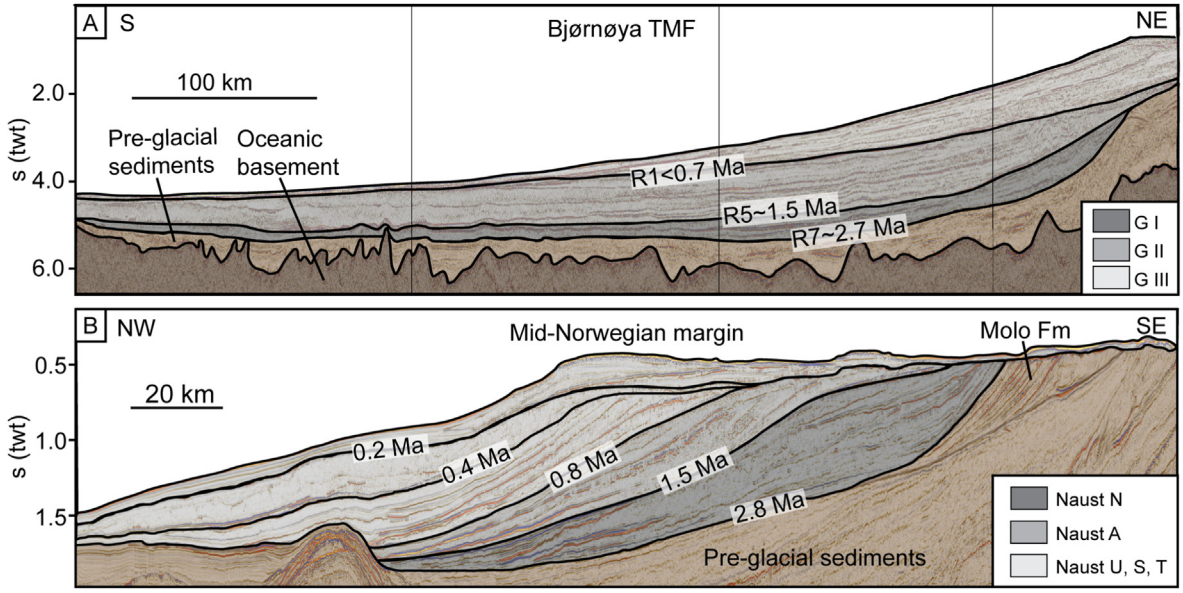

Fig. 2. (A) 2D multichannel seismic reflection profile, showing typical depositional pattern for the Bjørnøya TMF. Age estimates are from Laberg et al. (2010). GI-GIII: Identified Late Plio-Pleistocene seismic sequences (based on Fiedler and Faleide, 1996; Faleide et al., 1996). Location in Fig. 1A. **(B)** 2D multichannel seismic reflection profile showing typical character of the Late Plio-Pleistocene prograding wedge (Naust Fm) on the Mid-Norwegian margin. Chronostratigraphy is from Rise et al. (2010). Location in Fig. 1A.

and paleo-climate on glaciated margins (e.g., Sejrup et al., 2005). Investigations of these sedimentary systems can therefore contribute to our knowledge about glaciations prior to the last extensive glaciation (Marine Isotope Stage (MIS) 2).

Numerous studies have focused on mapping, describing and quantifying the glacier-derived Late Plio-Pleistocene sediment input to the different segments of the NE Atlantic continental margin (e.g., Solheim et al., 1996; Hjelstuen et al., 1996; Fiedler et al., 1996; Faleide et al., 1996; Rise et al., 2005; Ottesen et al., 2009, 2018; Laberg et al., 2012; Rydningen et al., 2016; Batchelor et al., 2017; Montelli et al., 2017). Results from these studies have provided new information on how the glaciated margin segments evolved in response to climate change, as documented in marine $\delta^{18}O$ isotope (Fig. 1B) (Lisiecki and Raymo, 2005) and ice rafted debris (IRD) records (e.g., Fronval and Jansen, 1996; Henrich and Baumann, 1994; Kleiven et al., 2002; Knies et al., 2009). Recently, Hjelstuen and Sejrup (2021) compiled a regional Late Plio-Pleistocene thickness map for the entire NE Atlantic-East Arctic Ocean margin, which as a basis, together with previously published sedimentation rate variations, was used to discuss the development of the EurIS.

In this study, we explore the Late Plio-Pleistocene sediment packages (Fig. 2) along the NE Atlantic margin further by compiling published sediment thickness information into new regional thickness maps for three time periods; the NHG Phase I (2.7–1.5 Ma), II (1.5–0.8 Ma) and III (0.8–0 Ma). In addition, catchment areas for identified depocenters have been suggested. Based on this, sediment volumes, sedimentation rates, glacial erosion rates and sediment yield values are estimated. This provides a basis for discussions of (i) the evolution of the NE Atlantic margin and (ii) EurIS spatial and temporal development through the Late Plio-Pleistocene.

2. Background

2.1. NE Atlantic margin morphology, oceanography and glaciation history

The continental shelves off Svalbard and Norway have a water depth of 200–500 m, a width of 50–150 km, and are characterized by relatively shallow banks separated by crosscutting troughs (Fig. 1A). The troughs terminate at the shelf break where TMFs, which are expressed as convex features in the bathymetric data, have built out (Fig. 1A). In the Barents Sea the water depth can reach more than 500 m in the troughs, while water depths of c. 50–300 m characterize the surrounding bank areas. The epicontinental North Sea has an average water depth of c. 50 m in the south and is gradually deepening to c. 200 m in the north. The most prominent feature in the North Sea is the 200–700 m deep and 50–100 km wide Norwegian Channel (Fig. 1A).

The present-day morphology of the NE Atlantic continental margin is to a large degree shaped by the repetitive build-up and disintegration of the EurIS throughout the Late Plio-Pleistocene (Sejrup et al., 2005; Lee et al., 2012). Previous studies have

suggested that the Yermak Plateau (Fig. 1A), and probably also the northern Barents Sea, were glaciated as early as c. 2.7 Ma (Knies et al., 2014; Lasabuda et al., 2018). Based on seismic data from the Albertini Trough north of Svalbard (Fig. 1A), Fransner et al. (2018a) suggested that ice streaming and shelf edge glaciations have occurred at least seven times during the Pleistocene in this region. The first shelf edge glaciation along the western Barents Sea-Svalbard margin is suggested to have occurred somewhat later, at c. 1.6 Ma (Solheim et al., 1998). From this time onwards, it has been suggested that grounded ice reached the western Barents Sea shelf edge at least eight times (Andreassen et al., 2004). This interpretation is also supported by enhanced IRD input to the marine realm (Butt et al., 2000) and the observation of glacigenic debris flows (GDFs), suggested to indicate shelf edge glaciations (King et al., 1996, 1998), in the sedimentary record (Vorren and Laberg, 1997; Solheim et al., 1998; Laberg et al., 2010). At c. 0.78 Ma the sedimentation rates along the western Barents Sea–Svalbard continental margin decreases significantly, indicating a less erosive KBSIS (Hjelstuen and Sejrup, 2021).

Based on analyses of a shallow boring from the Haltenbanken on the Mid-Norwegian margin (Fig. 1A), the first shelf edge glaciation in this region was initially suggested to have occurred at c. 1.1 Ma (Haflidason et al., 1991). More recently, observations of Mega-Scale Glacial Lineations (MSGLs) in 3D seismic data sets (Montelli et al., 2017), indicative of ice stream activity, in combination with a considerable build-out of the continental shelf (Ottesen et al., 2009), provide evidence that the ice margin reached the shelf edge in this region at the beginning of the Pleistocene (Ottesen et al., 2009; Montelli et al., 2017). IRD records (Jansen and Sjøholm, 1991) and observations of numerous iceberg ploughmarks (Montelli et al., 2018b; Newton et al., 2018) also document that ice sheets expanded out onto the Mid-Norwegian continental shelf in the Early Pleistocene. Throughout the last 0.6 Myr it has been suggested that shelf-edge-reaching ice sheets existed during MIS14, MIS12, MIS10, MIS8, MIS6 and MIS2 (Dahlgren et al., 2002; Hjelstuen et al., 2005; Sejrup et al., 2005).

In the northern North Sea, the identification of an Early Pleistocene glacifluvial channel system and GDFs are assumed to mark the onset of glaciation in this area (Løseth et al., 2020). These findings are supported by enhanced sedimentation rates (Anell et al., 2012), increased IRD input to the northern North Sea (Eidvin and Rundberg, 2001) and also by observations of iceberg ploughmarks in the central North Sea (Rea et al., 2018). These observations indicate that the FIS must have extended beyond the Norwegian coastline in the Early Pleistocene. Rea et al. (2018) also suggest that the BIIS extended beyond the British coastline during this time. More extensive ice sheets are suggested to have been built up in the North Sea region from c. 1.5 Ma (Batchelor et al., 2017; Reinardy et al., 2017), and during the last 0.5 Myr it has been suggested that ice sheets reached the shelf edge of the northern North Sea margin, and that the Norwegian Channel Ice Stream (NCIS) occupied the Norwegian Channel (Fig. 1A) during every glacial maximum (Sejrup et al., 2000; Nygård et al., 2005; Lee et al., 2012).

The build-up of large ice sheets is impacted by the interplay between oceanic and atmospheric processes, in which ocean circulation patterns play a vital role (e.g., Broecker et al., 1985; Ghil et al., 1987; Clark et al., 2002; Sejrup et al., 2005; Hodell and Channell, 2016). In the Nordic Seas (Fig. 1A) the ocean circulation pattern is at present characterized by warm surface water in the Norwegian Atlantic Current (NAC) flowing northwards along two branches towards the Fram Strait, the eastern of which is further branched into the Barents Sea (Orvik and Niiler, 2002; Tegzes et al., 2017) (Fig. 1A). At depths below 500 m, colder intermediate to deep water masses flow in a southern direction (Turrel et al., 1999; Hansen and Østerhus, 2000). Studies of iceberg ploughmark trajectories on the Mid-Norwegian margin show that the northward flowing configuration of the NAC has been largely consistent throughout the Pleistocene (Montelli et al., 2018b; Newton et al., 2018). Some short-lived intervals of reduced circulation have been suggested, and are related to major phases of iceberg discharge or meltwater pulses (Montelli et al., 2018b).

Cooling of the deep oceans during the Pleistocene have implications for atmospheric temperature and precipitation patterns, ice growth on the continents, and sea ice production (Tziperman and Gildor, 2003), and have also been suggested to have played a crucial role initiating both the NHG and the Mid-Pleistocene Transition (MPT) (Mudelsee and Schulz, 1997; Tziperman and Gildor, 2003; Hughes and Gibbard, 2018).

2.2. Late Plio-Pleistocene stratigraphy

During the last two decades, seismostratigraphical and chronostratigraphical frameworks have been established for segments of the NE Atlantic continental margin (Fig. 3). For the western Barents Sea margin, the seismostratigraphic framework comprises seven regional reflectors (R1-R7), that sub-divide the Cenozoic sedimentary package into one pre-glacial (G0) and three Late Plio-Pleistocene glacial (GI-GIII) units (Fig. 2A) (Fiedler and Faleide, 1996; Hjelstuen et al., 1996). This Late Plio-Pleistocene stratigraphic framework has been correlated to the recently established seismic stratigraphy (NB-3A, NB-3B and NB-3C; Fig. 3) of the

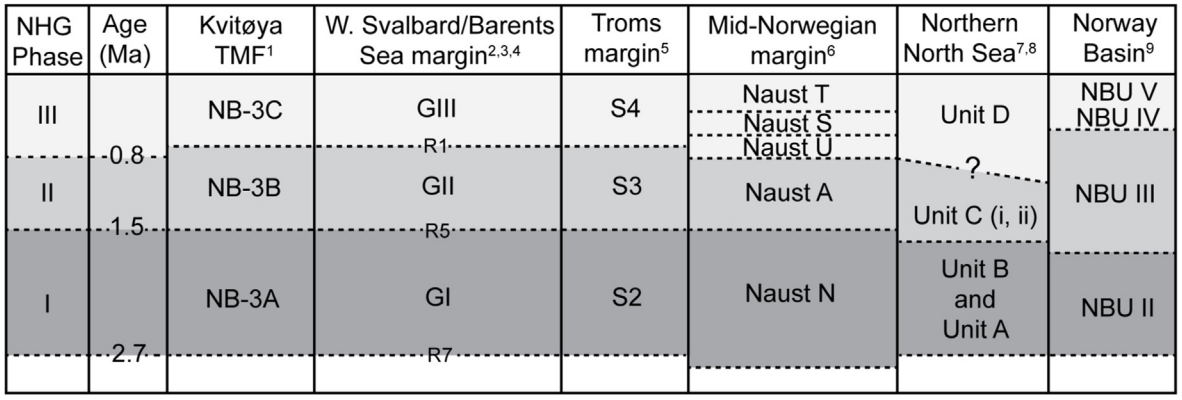

Fig. 3. Correlations of seismostratigraphic frameworks along the NE Atlantic Margin. TMF: Trough Mouth Fan. [1]Lasabuda et al. (2018), [2]Faleide et al. (1996), [3]Knies et al. (2009), [4]Laberg et al. (2010), [5]Rydningen et al. (2016), [6]Rise et al. (2010), [7]Ottesen et al. (2018), [8]Batchelor et al. (2018), [9]Hjelstuen et al. (2015).

Kvitøya TMF (Lasabuda et al., 2018), as well as other stratigraphic frameworks (Geissler and Jokat, 2004; Fransner et al., 2018b) on the northern Svalbard margin (Fig. 1A) and the TMF stratigraphy (S2–S4; Fig. 3) established for the Troms margin (Rydningen et al., 2016).

The current Late Plio-Pleistocene chronostratigraphy along the western Barents Sea-Svalbard margin is based on seismic ties of the regional sequence boundaries, i.e., R1, R5 and R7 (Figs. 2A and 3), to Ocean Drilling Program (ODP) boreholes. Age constrains are based on paleomagnetic and biostratigraphic data, where sequence boundaries R7 and R5 have an estimated age of 2.7 Ma and 1.5 Ma, respectively (Knies et al., 2009; Mattingsdal et al., 2014). The age of sequence boundary R1 (Fig. 2A) is more uncertain. However, based on an assessment of ages, data and methods used in previous works, this study follows Laberg et al. (2010) that set the age to be close to the Brunhes-Matuyama polarity reversal boundary (0.78 Ma; Gibbard et al., 2010). It should, however, be noted that younger ages have been suggested for sequence boundary R1 (Sættem et al., 1992; Faleide et al., 1996; Knies et al., 2009; Alexandropoulou et al., 2021).

On the Mid-Norwegian margin, the Naust Fm has been divided into five sub-sequences, N (oldest), A, U, S and T (youngest) (Rise et al., 2010; Ottesen et al., 2009; Montelli et al., 2017, 2018a) (Fig. 2B). The three oldest sub-sequences show a progradational pattern and are locally eroded on the inner shelf (Rise et al., 2006; Ottesen et al., 2009). Naust S and Naust T have a more aggradational character, and thus define a significant change in stratal architecture compared to the older sub-sequences (Dahlgren et al., 2002; Hjelstuen et al., 2004, 2005).

In order to determine the age of the Naust Fm, Eidvin et al. (2000) did a biostratigraphic correlation, tying the base Naust Fm to ODP boreholes on the Vøring Plateau (Fig. 1A). This attempt showed that the base Naust Fm coincides with enhanced input of IRD to the margin at around 2.75 Ma, as reported by Jansen and Sjøholm (1991). The upper boundary of Naust N has been given a tentative age of 1.5 Ma (Rise et al., 2006; Ottesen et al., 2014), whereas the age of base Naust U has been set to 0.8 Ma based on stratigraphic information (Rise et al., 2010). Dahlgren et al. (2002) did a seismic correlation to ODP Site 644 A, tying the youngest parts of the Naust Fm (Naust S and T) to the age-depth model by Henrich and Bauman (1994) that is based on oxygen isotope records and paleomagnetic data. From this, Naust S was dated to c. 0.4–0.2 Ma and Naust T is assumed to be younger than c. 0.2 Ma.

In the North Sea, two largely independent sub-basins developed during the Pleistocene; one in the southern and central North Sea, and one in the northern North Sea (Ottesen et al., 2014). In the Early Pleistocene it is suggested that fluvio-deltaic sedimentary processes dominated the depositional environment in the southern and central North Sea sub-basin, while erosional products from the uplifted Shetland Platform (Fig. 1A) and west Norway led to deposition of a sediment sequence dominated by prograding clinoforms in the northern North Sea sub-basin (Units A and B in Fig. 3; Huuse, 2002; Patruno et al., 2019; Ottesen et al., 2018). Unit C (Fig. 3) also consists of prograding clinoforms, but with deposition of GDFs as the dominant sedimentary process (Batchelor et al., 2017; Løseth et al., 2020). Following the initiation of the NCIS, glacial erosional products were transported northwards and deposited in the North Sea TMF (Sejrup et al., 1996; Nygård et al., 2005), forming the main depocenter of Unit D (Fig. 3).

Ottesen et al. (2018) correlated the base of Unit A (Fig. 3) to a surface in the southern North Sea that was dated to c. 2.6 Ma using paleomagnetic and biostratigraphic data (Kuhlmann et al., 2006). While Batchelor et al. (2017) indicated an age between 1.2 and 1.5 Ma for the top of Unit B, Ottesen et al. (2018) suggest an age slightly younger than 1.8 Ma (top Olduvai sub chron) for the same sequence boundary. The age of the prominent erosional surface that defines the base of Unit D is uncertain, but it has been linked to the first shelf edge glaciation in that area that, according to Sejrup et al. (1996), occurred at c. 1.1 Ma. Ottesen et al. (2014) suggested a somewhat younger age (c. 0.8 Ma), based on the identification of the Brunhes-Matuyama paleomagnetic boundary in North Sea boreholes.

The chronology of the sediment package in the Norway Basin (Fig. 1A) deep-sea area is poorly constrained. Hjelstuen and Andreassen (2015) correlated Late Pliocene-Early Pleistocene submarine slide deposits in this region to Slide W, released on the Møre continental slope. Slide W has an estimated age of 2.7–1.7 Ma (Solheim et al., 2005), and the slide debrites from this submarine slide seems to represent most of the unit defined as NBU II in the Norway Basin (Fig. 3). Likewise, the slide deposits in units NBU III (1.7–1.1 Ma) and NBU IV (c. 0.5 Ma), correlate to Slide U (Evans et al., 2005) and Slide S (Solheim et al., 2005), respectively. Unit NBU V represents the distal parts of the North Sea TMF (Nygård et al., 2005) and is suggested to be younger than 0.5 Ma.

3. Data and methods

3.1. Thickness maps and calculations

In this study Late Plio-Pleistocene thickness maps from the North Sea, the Norwegian margin, the western Barents Sea margin and the Svalbard margin have been compiled (Fig. 1A, Table S1 and Fig. S1 in Supplementary Data) into four regional thickness maps. Along the British-Irish North Atlantic and the eastern Arctic Ocean margins several TMFs have also been identified (e.g., Stoker et al., 2005; Vanneste et al., 2006; Owen and Long, 2016) (Fig. 1A). However, as it is commonly not possible to sub-divide the Late Plio-Pleistocene sediment packages in these regions into the three studied time periods (NHG Phases I-III), these TMFs, except for the Kvitøya TMF (Lasabuda et al., 2018), are not included in the present study. For each of the sediment depocenters identified in this study, catchment areas have been identified based on information on drainage pattern, topography, reconstructions of Pleistocene ice sheet extent (Batchelor et al., 2019) and ice divide and flowline models (Patton et al., 2016). For further details on thickness map compilation and definition of catchment areas, see Supplementary Data.

The ArcMap software, from Esri (https://www.esri.com), was used to estimate sediment volumes and sizes of depositional and catchment areas. Based on this information sedimentation rates, erosion rates, sediment discharge, sediment yield and net erosion have been calculated for each depocenter for each of the three studied time periods (Tables 1 and 2). In addition to this, we have also estimated the sediment volumes and depositional areas that are limited by the 200 m thickness contour (Table S2). In our calculations we follow previous studies of Dowdeswell et al. (2010) and Lasabuda et al. (2018), and assume an average sediment compaction of 20% when sediments are backstripped to their catchment area. This is done in order to compensate for higher pore volume in the depocenters, compared to the bedrock in the catchment area. For sediment density, we have used the average value of 2.2 g/cm^3 from Storvoll et al. (2005) which are based on well data covering the glacial sediment package on the Mid-Norwegian margin.

For the North Sea, and especially for its southern parts, a large part of the sediment volume deposited is assumed to be related to the Baltic and European river systems (e.g., Patruno et al., 2019). In order to estimate only the glacial sediment input, we make an assumption, based on previously published seismic data and thickness maps (Ottesen et al., 2018; Patruno et al., 2019), that 50%

of the total NHG Phase I and NHG Phase II sediment volumes in the North Sea are derived from southern and eastern sources not influenced by glacial processes. During NHG Phase III the fluvial input is assumed to have been considerably less (Ottesen et al., 2018; Gibbard and Cohen, 2015).

3.2. Uncertainties

There are uncertainties related to the estimates in this study. Firstly, it should be noted that while the published thickness maps from the western Svalbard-Barents Sea margin and Norway Basin (Fig. 1A) rely on a relatively few, coarsely gridded, 2D seismic data sets, the Norwegian continental margin and the North Sea have been extensively investigated using both 2D and 3D seismic data. This allows for a better constraint on the sediment distribution in the latter regions.

Contourite deposits may also introduce an uncertainty in the estimated values. Such sedimentary features are suggested to mainly be formed during interglacial periods, and they are commonly built by fine-grained sediments transported in, and deposited from, along-slope flowing oceanic currents (e.g., Rebesco et al., 2014). Thus, in our study the contourites are assumed not to have been sourced from the defined catchment areas (Fig. 4), but are sourced from sediments transported by the NE Atlantic oceanic current system (Fig. 1A). The uncertainties related to contourites are, however, considered to affect the estimates to a minor degree (<5%) as such sediment features are, so far, only observed in restricted areas along the NE Atlantic margin (Fig. S1) (Laberg et al., 2005; Rydningen et al., 2020).

Reworking of sediments (e.g., Bryn et al., 2005; Vanneste et al., 2006; Hjelstuen et al., 2007; Pope et al., 2018) may also impact the estimated values in this study. However, as the Late Plio-Pleistocene sediment package is divided into only three sub-units, this factor is assumed to be minimized because most of the reworked sediments are likely to originate from within the same defined sub-unit.

The uncertainty associated with the size of the defined catchment areas in this study becomes increasingly larger back in time. This is caused by the fact that topography, and thus drainage routes, will change over time due to various geologic processes, such as glacial erosion. Less is therefore also known about the nucleation and configuration of ice sheets during early glaciations in the Pleistocene compared to later glaciations. This applies in particular for the low-relief Barents Sea region which became submerged below sea level at c. 1 Ma (Zieba et al., 2017). The location of ice divides and flowline patterns have also been suggested to change during both the build-up and deglaciation of the EurIS during the late Weichselian (Dowdeswell et al., 2010; Hughes et al., 2014). Furthermore, previous studies have suggested that ice sheets stay at their maximum extent only for a relatively short period during a glaciation cycle (Elverhøi et al., 1998a; Svendsen et al., 2004; Nygård et al., 2007; Becker et al., 2018). Thus, the configuration of ice sheets and the extent of glacial erosion will vary within the defined catchment area through glacial cycles, and uncertainties related to this can be expected to increase back in time (Laberg et al., 2012).

Lastly, we find the chronostratigraphy to be reasonably well constrained along the western Barents Sea-Svalbard margin, for the younger part (<0.4 Ma) of the Mid-Norwegian margin Naust Fm and for the North Sea. Ages in the Norway Basin are more uncertain. Nonetheless, we suggest that the established chronostratigraphy of the three NHG Phase boundaries (Fig. 3), which are based on paleomagnetic and biostratigraphic correlations, are sufficient for the purpose of this study.

Despite the uncertainties, our results are assumed to provide a good first estimate, which enables an evaluation of Late Plio-Pleistocene source-to-sink processes along the NE Atlantic margin to be undertaken. In particular, the fact that the focus of this study is on large-scale sedimentation and erosion trends, and that the Late Plio-Pleistocene sediment package is divided into only three units, make us infer that uncertainties have a minor impact on the overall findings and conclusions of this study. An effort to quantify uncertainties has been carried out. In addition to assessing the spatial and temporal uncertainties in the catchment areas, we also included upper and lower values for sediment volumes, sediment density and sediment compaction. For further details, and minimum and maximum estimates of the values presented in this study (Tables 1 and 2, Fig. 5), see Supplementary Data.

4. Results

4.1. NHG Phase I

The Svalbard region had the highest sediment input along the entire NE Atlantic margin during NHG Phase I (Fig. 4A, Tables 1 and 2). The sediment input was especially high to the Storfjorden TMF, which increased the sediment thickness by 2000 m. Average sedimentation rates for the Storfjorden TMF during the NHG Phase I are estimated to be 73 cm/kyr (Table 1), which is more than 20 times higher than estimated Paleogene and Neogene sedimentation rates (Hjelstuen et al., 1996; Hjelstuen and Sejrup, 2021). These high sedimentation rates, combined with a relatively small catchment area, result in a high sediment yield, 1390 tons/km^2/yr, and an average erosion of 758 m in the Storfjorden TMF catchment area (Table 2). North of Svalbard, average sedimentation and erosion rates are estimated to 21 cm/kyr and 16 cm/kyr, respectively (Tables 1 and 2), for the NHG Phase I.

A sediment volume of 101 $\times$ 10^3 km^3 (2.2 $\times$ 10^{14} tons) is estimated deposited in the Bjørnøya TMF in NHG Phase I. This corresponds to an average sedimentation rate of 23 cm/kyr (Table 1), which is one order of magnitude higher than estimated sedimentation rates for the pre-glacial Cenozoic sediment package (Fiedler et al., 1996). An average erosion of c. 100 m is estimated in the catchment area of the Bjørnøya TMF. Both the sedimentation and erosion rates along the SW Barents Sea margin are considerably lower than the values estimated for the Storfjorden TMF (Tables 1 and 2).

On the Mid-Norwegian margin two depocenters developed in NHG Phase I, where the northern depocenter is up to 600 m thicker than the southern (Fig. 4A). The estimated average sedimentation (20 cm/kyr) and erosion rates (10 cm/kyr) on the Mid-Norwegian margin are comparable to the estimated values at the SW Barents Sea margin (Tables 1 and 2).

In the Norway Basin (Fig. 1A), a sediment thickness of up to 600 m is identified, which corresponds to an average sedimentation rate of 9 cm/kyr. It should be noted that this sediment package is interpreted to consist of slide debrites, sourced from slide events on the Møre margin during NHG Phase I (Hjelstuen and Andreassen, 2015).

In the North Sea, a northern and a southern depocenter, both reaching a maximum thickness of c. 500 m, characterize the sediment distribution (Fig. 4A). The sedimentation rates in this region are, however, relatively low (9 cm/kyr) compared to the Mid-Norwegian (20 cm/kyr) and the western Svalbard-Barents Sea margins (31 cm/kyr) (Table 1). As the glacial erosion products deposited in the North Sea during NHG Phase I were sourced from a, most likely, relatively small catchment area, confined to

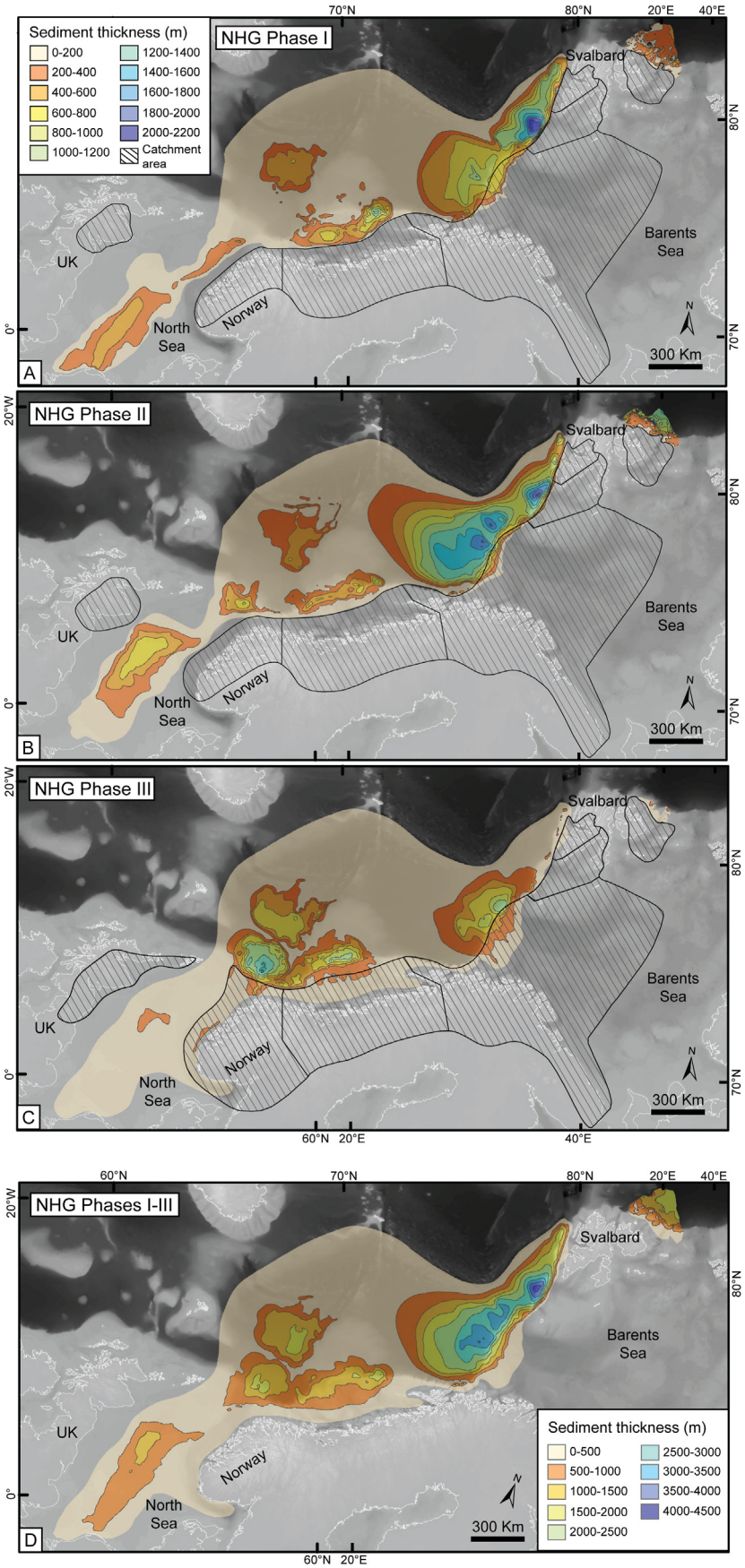

Fig. 4. Thickness maps in meters. **(A)** NHG Phase I (2.7–1.5 Ma), **(B)** NHG Phase II (1.5–0.8 Ma), **(C)** NHG Phase III (0.8–0 Ma) and **(D)** NHG Phases I-III (2.7–0 Ma). The legend in (A) also applies for (B) and (C).

Table 1
Estimated depositional areas, sediment volumes, sedimentation rates and sediment discharges for the major depocenters along the NE Atlantic margin. Columns marked with a dark grey color represent NHG Phase I, grey columns represent NHG Phase II and light grey columns represent NHG Phase III.

Region	Depositional area (10^3 km^2)			Sediment volume (10^3 km^3)			Sedimentation rate (cm/kyr)			Sediment discharge (10^6 tons/yr)		
Kvitøya TMF	44	28	8	11	17	1	21	87	11	20	53	2
Western Svalbard margin	35	27	38	21	10	2	50	52	8	38	31	7
Storfjorden TMF	68	53	50	60	40	7	73	109	16	109	127	18
Bjørnøya TMF	371	388	423	101	249	77	23	92	23	186	783	210
Mid-Norwegian margin	166	151	210	40	26	48	20	25	28	73	82	131
North Sea	224	243	384	24	30	29	9	18	9	44	95	79
North Sea TMF	96	100	106	6	11	53	5	15	62	11	34	145
Norway Basin	303	300	339	32	42	48	9	20	18	58	132	132
KBSIS	518	497	519	193	317	86	31	91	21	353	995	237
FIS/BIIS	792	794	1038	101	109	177	11	20	21	186	342	486
TOTAL	1311	1291	1557	294	425	263	19	47	21	539	1337	723

Table 2
Estimated catchment areas, eroded sediment volumes, sediment yields, erosion and erosion rates for the major depocenters along the NE Atlantic margin. Columns marked with a dark grey color represent NHG Phase I, grey columns represent NHG Phase II and light grey columns represent NHG Phase III.

Region	Catchment area (10^3 km^2)			Eroded sediment volume (10^3 km^3)			Sediment yield (tons/km^2/yr)			Erosion (m)			Erosion rates (cm/kyr)		
Kvitøya TMF	45	51	49	9	14	1	360	834	31	196	266	11	16	38	1
Western Svalbard margin	29	28	29	17	8	2	1057	874	179	576	278	65	48	40	8
Storfjorden TMF	63	63	63	48	32	5	1390	1602	228	758	510	83	63	73	10
Bjørnøya TMF	746	746	746	81	199	61	199	840	226	109	267	82	9	38	10
Mid-Norwegian margin	275	292	317	32	21	38	213	226	330	116	72	120	10	10	15
North Sea	141	201	386	19	24	23	249	375	163	136	119	59	11	17	7
North Sea TMF	141	201	386	5	9	42	61	135	300	33	43	109	3	6	14
Norway Basin	275	292	386	26	34	38	170	360	273	93	115	99	8	16	12
KBSIS	883	889	887	154	253	69	320	895	213	175	285	78	15	41	10
FIS/BIIS	415	494	704	81	87	141	358	555	553	195	177	201	16	25	25
TOTAL	1298	1383	1591	235	340	210	332	774	363	181	246	132	15	35	17

southwest Norway (Fig. 4A), the estimated erosion rates (14 cm/kyr) and average erosion (168 m) are rather high.

When comparing the northern (Svalbard-Barents Sea margin) and the southern (Norwegian margin) regions of the study area, it is clear that the sediment input to the NE Atlantic margin is much higher in the north (193×10^3 km^3) than in the south (101×10^3 km^3) (Fig. 5) during NHG Phase I. The average sedimentation rates are also about three times higher in the Svalbard-Barents Sea region compared to the values estimated in the south. However, sediment yield, net erosion and erosion rates are comparable in both regions during NHG Phase I as the northern catchment area is twice the size compared to the southern catchment area (Table 2, Fig. 5).

4.2. NHG Phase II

During NHG Phase II the sedimentation rates peak in every depocenter along the Svalbard-Barents Sea margin, and the average erosion rates almost triple compared to NHG Phase I (Tables 1 and 2). The Bjørnøya TMF had, by far, the highest sediment input, 249×10^3 km^3 (5.5×10^{14} tons). Further to the south, on the Mid-Norwegian margin, the Naust Fm continued to build out, creating a progressively wider continental shelf region (Fig. 2B and 4B). Average sedimentation rates along this margin segment were slightly higher (25 cm/kyr) than in the previous time period, while erosion rates are unchanged (10 cm/kyr) (Tables 1 and 2).

An increased sediment input is also observed both in the North Sea and in the North Sea TMF region during NHG Phase II (Table 1). The northern North Sea Basin is now the main region of deposition in the North Sea (Fig. 4B), and sediment yield values (375 tons/km^2/yr) and erosion rates (17 cm/kyr) in the North Sea catchment area are higher than the values estimated for the Mid-Norwegian margin (Table 2).

NHG Phase II represents the time interval of the NHG when the difference in sediment input between the northern and southern parts of the NE Atlantic margin was most prominent (Fig. 5). High average sedimentation rates (c. 100 cm/kyr) are estimated along the western Svalbard-Barents Sea margin, whereas the average sedimentation rates along the Mid-Norwegian margin and in the North Sea are moderate (c. 20 cm/kyr). Because of the high sedimentation rates in the north, a three times higher sediment volume was deposited along the Svalbard-western Barents Sea compared to the Norwegian margin during NHG Phase II. Average erosion rates are estimated to 41 cm/kyr and 25 cm/kyr for the northern and southern region of the study area, respectively. During NHG Phase II a total sediment volume of 425×10^3 km^3 was deposited along the NE Atlantic margin. Thus, NHG Phase II represents the time interval during the entire Late Plio-Pleistocene time period when, the NE Atlantic continental shelf and slope received the highest amount of erosion products (Fig. 5).

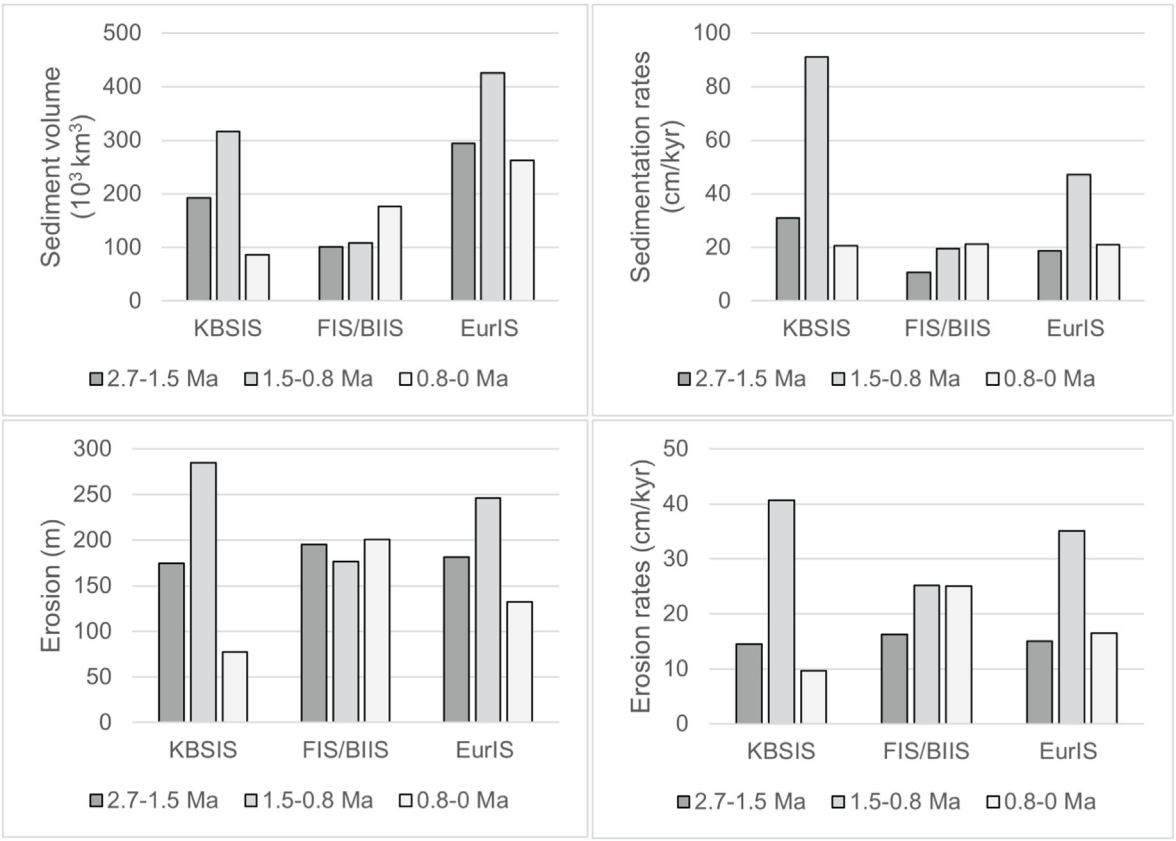

Fig. 5. Histograms showing temporal and spatial variations in sediment volumes, sedimentation rates, average vertical erosion and erosion rates in the defined catchment areas during NHG Phases I-III for the FIS/BIIS, KBSIS and EurIS.

4.3. NHG Phase III

During NHG Phase III the sediment yield values along both the northern and western Svalbard margin dropped significantly, compared to NHG Phases I and II. Thus, both the erosion in the catchment area and the sedimentation rates in the depositional area were low during this time period (Tables 1 and 2, Fig. 4C). The only area within the Barents Sea region where the sedimentation rates are somewhat sustained in NHG Phase III, compared to NHG Phase II, is within the Bjørnøya TMF (23 cm/kyr). The erosion rates in the catchment area of the Bjørnøya TMF are, however, at the same level as the erosion rates estimated for the Storfjorden TMF catchment area (10 cm/kyr).

On the Mid Norwegian margin, on the other hand, the estimated sedimentation rates are the highest during the entire Late Plio-Pleistocene (28 cm/kyr) in NHG Phase III. Average sedimentation rates of >60 cm/kyr are estimated in the other major depocenter along the Norwegian margin; the proximal part of the North Sea TMF. Despite the substantial sediment input to the marine realm, average vertical erosion is relatively low (c.100 m) in the catchment areas. The low value is related to the large catchment area that has been suggested (Table 2).

A considerable volume of sediments, 48 $\times$ 10^3 km^3 (1.1 $\times$ 10^{14} tons), was deposited in the Norway Basin during NHG Phase III, giving sedimentation rates in the order of 18 cm/kyr. The sediments deposited in the Norway Basin during this time period consist mainly of GDFs, sourced from the upper part of the North Sea TMF (Nygård et al., 2005). Much of these deposits are likely to have originated from the southern Scandinavian catchment area. However, some of the sediments deposited are also associated with submarine slide debrites, related to submarine slides along the neighboring continental slopes (Haflidason et al., 2005; Nielsen et al., 2007). At the beginning of NHG Phase III the North Sea Basin was mainly filled (Ottesen et al., 2018), and the deposition pattern became more widespread and uniform, with a larger depositional area and with sediment thicknesses commonly less than 200 m (Fig. 4C). Sedimentation rates (9 cm/kyr) and erosion rates (7 cm/kyr) are low in the North Sea compared to the rate estimates for NHG Phase II (Tables 1 and 2).

When comparing the erosion estimates in the FIS/BIIS and KBSIS catchment areas, the erosion is considerably higher in the south (25 cm/kyr) than in the north (10 cm/kyr) (Fig. 5) during NHG Phase III. However, this is not related to increased erosion in the south, which remains unchanged since NHG Phase II, but rather a dramatic decrease of erosion in the KBSIS catchment area from NHG Phase II to III (Tables 1 and 2). This shows that NHG Phase III is characterized by a distinct change in deposition pattern along the NE Atlantic margin from the NHG Phase II. That is, the FIS/BIIS catchment area became the dominant source area along the NE Atlantic margin. A sediment volume of 177 $\times$ 10^3 km^3 has been deposited along the Norwegian margin and in the North Sea since c. 0.8 Ma, whereas 86 $\times$ 10^3 km^3 of sediments were deposited along the marine margin of the KBSIS (Fig. 5, Table 1).

5. Discussion

As glacial influence can cause up to several orders of magnitude increase in the sedimentation rates (Table S3; e.g., Hjelstuen et al., 1996; Anell et al., 2012), these can also be used as an indicator of ice sheet extent and dynamics. Shelf edge glaciations are in this sense

important events, since it is during these relatively short periods through a glacial cycle that much of the sediment are deposited on the continental slope and shelf edge progradation occurs (Elverhøi et al., 1998b; Dahlgren et al., 2005; Stoker et al., 2005). Laberg et al. (2009) estimated a sediment discharge as high as 103×10^6 tons/yr for the Vestfjorden Ice Stream during the period from 26 to 18 kyr, and Nygård et al. (2007) estimated 1100×10^6 tons/yr for a period with high GDF activity in front of the NCIS during the Last Glacial Maximum. The latter value equals an average sedimentation rate of 3600 cm/kyr. In comparison, glacimarine sedimentation rates are typically c. 70 cm/kyr along the Norwegian margin, while interglacial sedimentation rates in the same region are estimated to c. 10 cm/kyr (Table S3; Haflidason et al., 1998; Laberg et al., 2018).

5.1. EurIS development 2.7–1.5 Ma (NHG Phase I)

During NHG Phase I, high sedimentation rates are observed along the northeastern margin of the KBSIS (Figs. 5 and 6A). The average sedimentation rates at the Storfjorden TMF (73 cm/kyr) and at the western Svalbard TMFs (Fig. 1A) (50 cm/kyr) are comparable to ice proximal glacimarine environments during the last glaciation (Table S3; Hjelstuen et al., 2004; Lekens et al., 2005; Laberg et al., 2018). Given the fact that NHG Phase I includes several warm intervals (Lisiecki and Raymo, 2005), that may be characterized by low sedimentation rates (Table S3), glacimarine environments alone seem insufficient to explain the estimated high sedimentation rates at the marine margin of the KBSIS. Thus, periods of shelf edge glaciations and probably ice stream activity are suggested to be necessary to account for these high estimated sedimentation rates (Fig. 6A). IRD pulses recorded in ODP sites, both at the Yermak Plateau (Fig. 1A) and along the western Svalbard margin (Butt et al., 2000; Knies et al., 2009), also support ice expansion into the marine realm. Identification of GDFs and shelf edge progradation along the northern Svalbard margin (Mattingsdal et al., 2014; Fransner et al., 2018a; Lasabuda et al., 2018) and development of several western Svalbard TMFs (Solheim et al., 1998; Sarkar et al., 2011) (Fig. 1A) indicate shelf edge glaciations and ice stream activity in this region during NHG Phase I.

Sedimentation and erosion rates in the Bjørnøya TMF region are moderate compared to the estimates for the TMFs further north (Tables 1 and 2). Based on grain size distribution in well data, glacial influence in this region has been suggested (Knies et al., 2009). However, the extent of the Early Pleistocene KBSIS in the SW Barents Sea has been poorly constrained. Laberg et al. (2010) suggested that the Early Pleistocene sediments along the SW Barents Sea margin primarily consist of distal glacimarine sediments sourced by glacifluvial processes from a land-terminating ice sheet. Knies et al. (2009) suggested a moderate-sized KBSIS during the earliest Pleistocene, with short-term glacial expansions beyond the coastline of the uplifted western Barents Sea, whereas Hjelstuen and Sejrup (2021), on the other hand, proposed shelf edge glaciations and that KBSIS merged with the FIS towards the end of NHG Phase I.

Based on the rate estimates in this study, periodic shelf edge glaciations in the Bjørnøya TMF region probably occurred during NHG Phase I (Fig. 6A). Given that much of the Bjørnøya TMF catchment area has been suggested to have been lowlands, above sea level, and located in a polar region (Vorren et al., 1991; Butt et al., 2002; Zieba et al., 2017), fluvial and glaciofluvial processes alone seem insufficient to explain a sediment yield of 200 tons/km^2/yr. This is further supported by studies on large Arctic river systems that are characterized by sediment yield values that are an order of magnitude less (Milliman and Syvitski, 1992; Syvitski, 2002; Gordeev, 2006) than those values which are estimated for the Bjørnøya TMF catchment area (Table 2). Furthermore, from fluvial basins on Svalbard, Svendsen et al. (1989) estimated erosion rates to be one order of magnitude less than what is found for the Bjørnøya TMF catchment area. Recently, Harishidayat et al. (2020) have also identified MSGLs close to the Pliocene-Pleistocene boundary along the SW Barents Sea margin, suggesting that ice streams have been active periodically in this region during NHG Phase I.

It is likely that shelf edge glaciations occurred along the FIS margin during NHG Phase I (e.g., Ottesen et al., 2009). Our compilation also supports this as the sedimentation and erosion rates on the Mid-Norwegian margin are comparable to rates estimated during NHG Phases II and III (Tables 1 and 2), when shelf edge glaciations are suggested to have occurred (Rise et al., 2005; Sejrup et al., 2005; Ottesen et al., 2009; Montelli et al., 2017). Furthermore, in the Late Pliocene the shelf edge was located up to 150 km more landward than at present (Fig. 2B). This suggest that the marine margin of the FIS would have terminated at the shelf edge only 50–80 km from the present-day Norwegian coastline. A considerable seaward progradation of the Mid-Norwegian continental shelf, up to 100 km, in the Early Pleistocene (Ottesen et al., 2009), in addition to the identification of MSGLs close to the shelf edge and near the base of the Naust Fm (Montelli et al., 2017), indicate that shelf edge glaciations occurred along the Mid-Norwegian margin during NHG Phase I. In the North Sea catchment area, similar erosion rates as those estimated for the Mid-Norwegian margin catchment area are identified, indicating that similar glacial processes existed in the North Sea region. The observation of Early Pleistocene GDFs (Løseth et al., 2020) and ploughmarks (Rea et al., 2018), as well as several generations of MSGLs (Rea et al., 2018), also indicate periodic presence of an ice sheet in this region.

The data presented here, including both rate estimates and evidence of grounded ice on the continental shelf (Montelli et al., 2017; Rea et al., 2018; Løseth et al., 2020), indicates that episodic large-scale shelf edge glaciations may have occurred along the entire NE Atlantic margin during NHG Phase I (Fig. 6A). It is also a possibility that the individual ice sheets, comprising the EurIS coalesced towards the end of NHG Phase I, as previously has been suggested by Hjelstuen and Sejrup (2021) and Rea et al. (2018). Although the KBSIS delivered twice as much sediment to the continental slope during NHG Phase I compared to FIS/BIIS (Fig. 6D), similar average erosion rates of c.15 cm/kyr characterize the catchment area in both regions. For comparison, global erosion rates during the Cenozoic prior to the NHG are suggested to be < 2 cm/kyr (Willenbring and Blanckenburg, 2010).

5.2. EurIS development 1.5–0.8 Ma (NHG Phase II)

During NHG Phase II, the entire NE Atlantic continental margin experienced an increased input of glacial erosion products compared to NHG Phase I (Tables 1 and 2, Fig. 6D). Along the marine margin of the KBSIS the sedimentation rates almost tripled (c. 100 cm/kyr) compared to NHG Phase I. This rate increase is likely related to enhanced erosion in the catchment area of the Bjørnøya TMF (Table 2). However, changes in the size of the catchment area may also have influenced the rates. This large increase in erosion probably relates to the development of a prominent ice stream in the Bjørnøya Trough, which is also evidenced by MSGLs (Waage et al., 2018; Harishidayat et al., 2020), mega blocks of consolidated sediments and GDFs deposited on the continental slope (Andreassen et al., 2007; Laberg et al., 2010). In the catchment areas of the Storfjorden TMF and the western Svalbard TMFs, erosion rates for NHG Phase II are comparable to the erosion rates which were estimated for NHG Phase I (Table 2). This indicates that

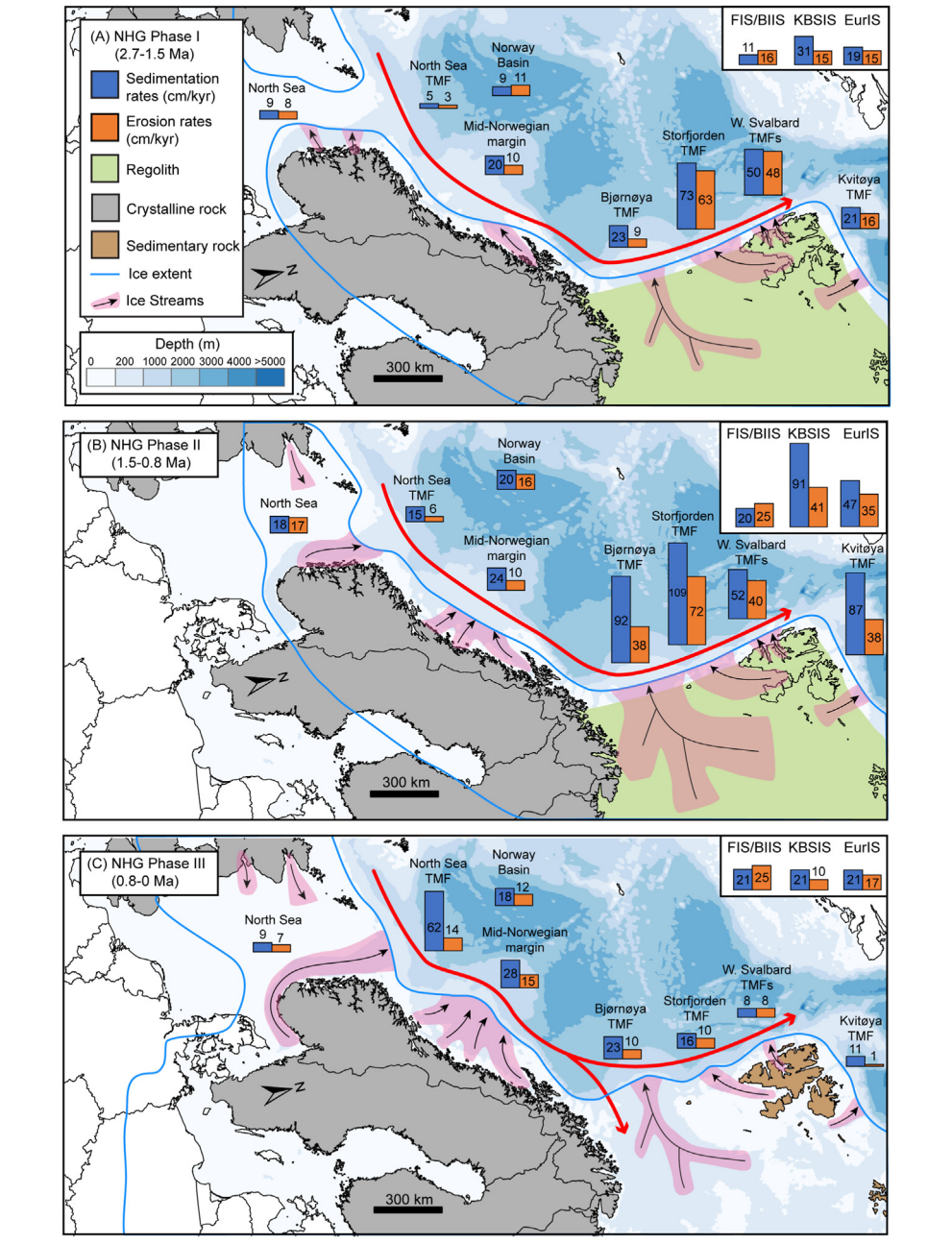
(A) NHG Phase I
(2.7-1.5 Ma)
Sedimentation rates (cm/kyr)
Erosion rates (cm/kyr)
Regolith
Crystalline rock
Sedimentary rock
Ice extent
Ice Streams
Depth (m)
0 200 1000 2000 3000 4000 >5000
300 km
FIS/BIIS KBSIS EurIS
North Sea
North Sea TMF
Norway Basin
Mid-Norwegian margin
Storfjorden TMF
W. Svalbard TMFs
Bjørnøya TMF
Kvitøya TMF
(B) NHG Phase II
(1.5-0.8 Ma)
(C) NHG Phase III
(0.8-0 Ma)

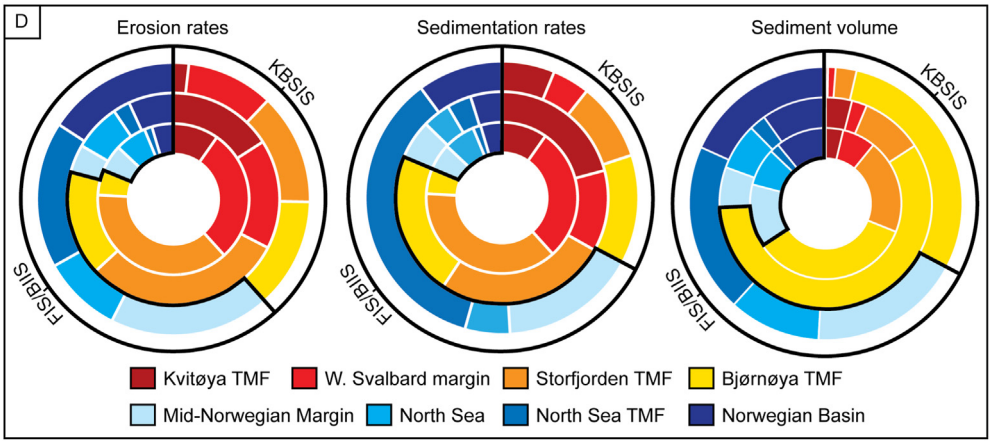
D
Erosion rates
Sedimentation rates
Sediment volume
KBSIS
FIS/BIIS
Kvitøya TMF
W. Svalbard margin
Storfjorden TMF
Bjørnøya TMF
Mid-Norwegian Margin
North Sea
North Sea TMF
Norwegian Basin

extensive ice sheets and ice streaming persisted during NHG Phase II in this region. Recurrent shelf edge glaciations during this period have also been inferred based on observation of several erosional unconformities on the shelf, and debris flow deposits on the continental slope (Faleide et al., 1996; Solheim et al., 1996, 1998). This ice sheet expansion is, furthermore, evidenced by high IRD accumulation rates on the western Barents Sea margin and the Yermak Plateau (Knies et al., 2009).

In the time period 1.5–0.8 Ma, glacial erosion intensified in the FIS/BIIS catchment area as well. However, the increase is somewhat less than what is identified for the Barents Sea. Increased erosion rates are most evident in the North Sea and are probably related to the build-up of larger ice volumes (Sejrup et al., 2005; Ottesen et al., 2018). On the Mid-Norwegian margin, only a moderate increase in sedimentation rates is identified, whereas the sediment yield and erosion rates are on the same level as in NHG Phase I (Tables 1 and 2). It is therefore plausible that the catchment area of the Mid-Norwegian margin was characterized by similar extent of glacial erosive processes during NHG Phases I and II.

Increased ice stream activity in the FIS and the BIIS during NHG Phase II is also evidenced by seismic data, where numerous generations of MSGLs are observed both at the Mid-Norwegian margin (Ottesen et al., 2009; Montelli et al., 2017) and in the North Sea (Buckley, 2017; Rea et al., 2018). The orientation of the MSGLs in the North Sea indicate that ice streams originate from both the southern Norway and the British Isles and reached as far south as c. 57°N. Other evidence regarding more extensive glaciations during NHG Phase II includes increased input of IRD along the marine margin of the FIS/BIIS (Jansen and Sjøholm, 1991; Henrich and Baumann, 1994; Thierens et al., 2012), and more frequently occurring iceberg ploughmarks in both the North Sea (Dowdeswell and Ottesen, 2013; Rea et al., 2018) and at the Mid-Norwegian margin (Montelli et al., 2018b; Newton et al., 2018).

NHG Phase II appears to be the most erosive period in the EurIS history (Fig. 5). A sediment volume of 425×10^3 km^3 was deposited along the marine margin of the EurIS during this period, resulting in average sedimentation rates of 47 cm/kyr (Table 1). This is an increase in sedimentation rate close to 150% compared to NHG Phases I and III. This shows that the total sediment output from the EurIS was highest prior to the development of 100 ka glaciation cycles (e.g., Lisiecki and Raymo, 2005). Our compilation therefore supports that extensive ice sheets existed in NHG Phase II and that the KBSIS, FIS and BIIS merged during peak glaciations. Widespread ice stream activity also seems to have occurred along the NE Atlantic margin during this time period (Fig. 6B). This study also shows that the erosion was most significant in the Barents Sea-Svalbard region (Table 2), indicating large spatial heterogeneity in the EurIS erosive capacity during the late early Pleistocene.

5.3. EurIS development 0.8–0 Ma (NHG Phase III)

A dramatic reduction in the glacial sediment input along the marine margin of the KBSIS took place in the most recent part of the Pleistocene (Table 1). Less than 10×10^3 km^3 of glacial sediments were deposited in total at the Storfjorden TMF, the western Svalbard TMFs and the Kvitøya TMF during this time period. At the Bjørnøya TMF the sediment volume deposited decreased from 249×10^3 km^3 in NHG Phase II to 77×10^3 km^3 in NHG Phase III. The low erosion rates in the catchment areas are not related to restricted ice sheet extent, as it is well established that recurrent shelf edge glaciations occurred along the KBSIS marine margin after 0.8 Ma (e.g., Faleide et al., 1996; Sejrup et al., 2005; Laberg et al., 2010; Waage et al., 2018; Harishadayat et al., 2020). Observation of MSGLs in the sedimentary succession also suggests that repeated ice stream activity occurred (Andreassen et al., 2007; Bellwald et al., 2019) (Fig. 6C). The apparent conflict between large ice extent and low erosion rates in the KBSIS region may be related to factors such as the submergence of the Barents Sea (see Section 6).

On the Mid-Norwegian margin the sediment input doubled, while it increased fivefold for the North Sea TMF during NHG Phase III (Table 1). Thick sequences of GDFs within the North Sea TMF indicate recurrent ice stream activity in the Norwegian Channel (Nygård et al., 2005; Bellwald et al., 2020), whereas identification of MSGLs on the Mid-Norwegian continental margin indicate intense ice stream activity in this region (Montelli et al., 2017) (Fig. 6C). Despite the large volumes of sediments deposited on the North Sea TMF and the Mid-Norwegian continental margin, the overall sediment yield in the FIS/BIIS catchment area remain unchanged from NHG Phase II to NHG Phase III. Thus, the increase in glacial sediment volume delivered to the margin in NHG Phase III does not seem to be mainly associated with more intense glacial erosion (Table 2), but rather that the FIS catchment area increased considerably in size (Fig. 4). The increased size in catchment area relates to the initiation of the NCIS which drained a large part of central Scandinavia (Sejrup et al., 1996; Hjelstuen et al., 2012; Patton et al., 2016). Thus, the erosive nature of the ice sheets covering Scandinavia and the British Isles during NHG Phase III, was similar to the ice sheets that existed during NHG Phase II.

During NHG Phase III, the main difference in character of the EurIS from the two previous phases, is that the FIS/BIIS became the main contributor of glacial sediment input to the NE Atlantic margin (Fig. 6D). This indicates that a major shift in the glaciological setting of the EurIS occurred between NHG Phase II and III. Still, it is suggested that large ice volumes and shelf edge glaciations occurred along the entire marine margin of the EurIS during NHG Phase III (Fig. 6C), as also evidenced by previous studies of IRD records in the Nordic Seas (Jansen et al., 2000; Knies et al., 2009) and by ice stream activity on the shelf (Andreassen et al., 2007; Montelli et al., 2017; Rea et al., 2018).

6. Wider implications for Pliocene climate and Pleistocene EurIS development

Our compilation of sediment thicknesses (Fig. 4) along the NE Atlantic margin suggests a significant change in topography/bathymetry and land-sea configuration throughout the Late Plio-Pleistocene. Especially in the Barents Sea region, the average vertical erosion in the Bjørnøya TMF catchment area are 175, 285 and 78 m, for NHG Phases I, II and III, respectively (Table 2). As uplift in the Barents Sea has been suggested to be far less than erosion by model simulations (Fjeldskaar and Amantov, 2018), this indicates that the Barents Sea was subaerial during the Early Pleistocene, as also suggested in previous studies (Vorren et al., 1991; Butt et al., 2002; Hill, 2015; Zieba et al., 2017) (Fig. 6). Accordingly, we suggest that the western Barents Sea was subaerial, and the eastern Nordic Seas (Fig. 1A) was deeper than present-day prior to the Pleistocene. This indicates that a period that is used as an analog for future climate scenarios, the Mid Pliocene warm period (c. 3 Ma)

Fig. 6. Conceptual model summarizing suggested maximum ice sheet extent and ice stream activity during **(A)** NHG Phase I, **(B)** NHG Phase II and **(C)** NHG Phase III. The bar charts show sedimentation rates (orange) and erosion rates (blue) along the marine margin of the EurIS. Red arrows indicate northwards flowing North Atlantic surface water (from Orvik and Niiler, 2002). **(D)** Pie charts showing relative variations in erosion rates, sedimentation rates and sediment volume for each region along the NE Atlantic margin during NHG Phases I-III. The inner, middle and outer circles represent NHG Phase I (2.7–1.5 Ma), NHG Phase II (1.5–0.8 Ma) and NHG Phase III (0.8–0 Ma), respectively. (For interpretation of the references to color in this figure legend, the reader is referred to the Web version of this article.)

(Haywood et al., 2016b), is characterized by a setting that is substantially different from present day in the Nordic Seas-Arctic Ocean region (Fig. 1A). When the Barents Sea was subaerial, this region would have been more exposed to glacial nucleation and erosion. While the Barents Sea became submerged below sea level in late NHG Phase II (Zieba et al., 2017), erosion would initiate only after ice sheets were large enough for marine ice shelves to become grounded. This suggests that subglacial erosion occurred in a shorter time interval during glacial cycles in comparison with that occurred when the Barents Sea region was terrestrial.

A long-standing challenge for Pliocene climate simulation is to account for the large underestimation of simulated surface warming in the Nordic Seas in comparison to sea surface temperature (SST) proxy records (Dowsett et al., 2013). Previous modelling studies have proposed that geographic changes in the Kara-Barents Sea (Fig. 1A) are of great importance for surface temperature change in the Nordic Seas (e.g., Hill, 2015). That is, changing the Barents Sea from a marine to a subaerial setting can give rise to evident warming in the Nordic Seas (Hill, 2015). Nevertheless, this geographic change has so far not been well considered in the Pliocene Modelling Intercomparison Project (PlioMIP) (Haywood et al., 2016a, b), a flagship project for Pliocene climate modelling. One potential reason for this overlook is due to the lack of quantitative information for erosion amounts from the KBSIS catchment areas, which are used to quantify paleogeography in the Kara-Barents Sea regions through time. Our compilation fills this gap and confirms that the change from subaerial to submerged conditions in the Kara-Barents Sea regions occurred during the Mid Pleistocene, suggesting the existence of subaerial Barents Sea shelves during the Pliocene. Therefore, taking into account this paleogeographic change in PlioMIP protocol bears the potential to reconcile the data-model mismatch (Dowsett et al., 2013), since land is characterized by a lower heat capacity than sea water and hence more sensitive to increasing solar/radiative forcing.

During the Pleistocene, one significant feature of glacial-interglacial (G-IG) cycles is the MPT (1.2–0.6 Ma), when the periodicity of G-IG cycles shifted from 40-kyr to 100-kyr without systematic changes in orbital configurations (Berends et al., 2021). Changes in ice sheet dynamics associated with removal of a regolith cover in North America have been proposed to play a role during the MPT (Clark and Pollard, 1998; Willeit et al., 2019; Yehudai et al., 2021). Based on our compilation, it appears that during NHG Phase II (1.5–0.8 Ma) the KBSIS basal conditions experienced a significant change – i.e., change from subaerial to submarine. In addition, the dramatic decrease in erosion rates (>75%) observed along the KBSIS marine margin from NHG Phase II to NHG Phase III, suggests that an easily erodible regolith cover was not present any more in the KBSIS catchment area during NHG Phase III. These lines of evidence indicate the existence of a thick regolith layer in the Kara-Barents Sea region before NHG Phase III, which was gradually eroded by Eurasian glaciation during the Early and Mid Pleistocene.

In addition to its impacts on ice sheet dynamics *per se*, the associated paleogeographic change also play a critical role in moisture source for ice sheet growth by modulating atmosphere-ocean circulation, probably affecting Northern Hemisphere glaciation history. Oceans are the main moisture source for precipitation over land. During NHG Phase I moisture mainly came from the Nordic Seas when the Kara-Barents Sea regions were subaerial for ice sheet nucleation, as supported by high sedimentation rates in TMFs along the KBSIS region (Table 1). When the Kara-Barents Sea regions gradually became submerged during the NHG Phase II, the moisture source extended eastwards to the Kara-Barents Sea, shortening its distance to the northwestern Siberian region where an ice sheet could be promoted by enhanced snowfall prior to the development of a marine-based ice sheet in the Kara-Barents Sea. This altered Eurasian glaciation history might further impact North American glaciation by modulating circum-polar atmospheric circulation as proposed by Zhang et al. (2020). Therefore, the removal of regolith cover in the KBSIS region, by shifting the Kara-Barents Sea regions from subaerial to submerged conditions, might alter the evolution of the NHG, eventually accounting for the occurrences of the MPT, although there exists evident nonlinearity in ice-sheet nucleation/development as revealed by Weichselian glaciation (Larsen et al., 2006).

Based on our results, we further suggest a thin or negligible regolith cover present in the FIS/BIIS catchment area since its erosion rates were almost unchanged through time (Table 2). In addition, variations in type of eroded bedrock are likely to have an impact on sedimentation pattern along the marine margin of the EurIS. Wellner et al. (2001), by studying major drainage outlets of the Antarctic Ice Sheet, show that ice flows over sedimentary rocks can produce larger amounts of sediments than ice flows over crystalline rocks. The glacially eroded bedrock in Scandinavia, which is mainly crystalline, is therefore more resistant to erosion than the sedimentary bedrock in the Barents Sea and on Svalbard (Lasabuda et al., 2018, 2021). Thus, higher erosion rates can be expected from the KBSIS catchment areas compared to the catchment areas of the FIS, based on bedrock properties. Since sedimentary bedrock tends to be more consolidated with depth and age (van Hinte, 1978), the sedimentary bedrock eroded by the KBSIS during NHG Phase III may be more resistant to erosion compared to the substrate that was eroded during the previous NHG phases, as these rocks have been subjected to deeper burial. However, according to velocity analyses of eroded rocks in the Storfjorden (Hjelstuen et al., 1996) and Bjørnøya TMFs (Fiedler et al., 1996) catchment areas, only minor changes in the bedrock character have occurred during the Pleistocene. Variations in bedrock consolidation are, therefore, assumed to be less important for the erosion rate.

The erosive capacity of ice sheets is highly dependent on their basal thermal regime (Dowdeswell and Siegert, 1999; Kleman et al., 2008), which is controlled by glaciological factors like surface temperature of the ice, ice thickness and geothermal heat flux (Hooke, 1977). A cold-based regime, with limited erosion capacity, has been proposed for large regions of both the FIS and the Laurentide Ice Sheet during the Last Glacial Maximum (Kleman and Hättestrand, 1999). It is therefore reasonable to assume that similar, or even more pronounced, cold-based conditions existed for parts of the KBSIS during NHG Phase III, which received less insolation than the FIS. In fact, extensive preservation due to frozen subglacial conditions have been suggested in the Barents Sea during the Last Glacial Maximum based on a thermomechanical modelling study (Patton et al., 2016). A setting where erosion mainly occurs within troughs due to ice stream activity, while little erosion occurs on surrounding banks, has already been suggested along the marine margin of the KBSIS during the Late Pleistocene (Ottesen, 2005; Laberg et al., 2012). The lack of erosion on the banks can be related to cold based ice conditions in these areas, caused by e.g., thinner ice on the banks after the reconfiguration of the KBSIS following the submergence of the Kara-Barents Sea region. Thus, although removal of regolith and eastward shift in ice sheet nucleation are suggested to be the main cause explaining the large decline in erosion rates in the KBSIS catchment area from NHG Phase II to NHG Phase III, increased extent of cold-based ice may also have been a contributing factor.

In summary, the late Cenozoic variations in glacial sediment supply to the NE Atlantic margin, as identified in this study, is closely related to climatic impacts, large-scale geomorphologic evolution and NHG processes. The amounts of erosional products delivered to the marine margin of the EurIS are also strongly related

to the size and location of the catchment areas. This is inferred in particular from the changes in the FIS catchment area, while the proposed eastward shift in ice nucleation from NHG Phase II to NHG Phase III might indicate the same for the KBSIS. The apparent coincidence between glacial intensification and reconfiguration of sediment distribution from NHG Phase II to NHG Phase III, together with other lines of evidence (Pena and Goldstein, 2014; Lear et al., 2016; Chalk et al., 2017; Barker et al., 2021) suggests that different components of the Earth System are closed coupled while change in paleogeography might be a key player that stimulating a chain of internal feedbacks (e.g., ocean circulation change, carbon cycle, ice sheet dynamics and geometry, etc. (Berends et al., 2021 and references therein)), which eventually accounts for the observed climate changes across the MPT. In the future, modelling by the Earth System model with interactive ice sheet dynamics and carbon cycles is required to test this chain of processes.

7. Conclusions

In this study previously published results from the NE Atlantic margin have been used to compile regional thickness maps for the time periods 2.7–1.5 Ma, 1.5–0.8 Ma, 0.8–0 Ma and 2.7–0 Ma. Based on these thickness maps and the identification of catchment areas, quantitative estimates of volume, sedimentation rates, erosion rates, sediment discharge, sediment yield and net erosion have been calculated. The main conclusions from this study are:

- The sediment input along the marine margin of the EurIS was highly variable during the Late Plio-Pleistocene. During NHG Phases I (2.7–1.5 Ma), II (1.5–0.8 Ma) and III (0.8–0 Ma) sediment volumes of 294 $\times$ 10^3 km^3, 425 $\times$ 10^3 km^3 and 263 $\times$ 10^3 km^3 were deposited along the marine margin of the EurIS, respectively.
- Average vertical erosion rates in the EurIS catchment area during Late Plio-Pleistocene are estimated to have varied from 15 cm/kyr in NHG Phase I, to 35 cm/kyr in NHG Phase II and to 17 cm/kyr during NHG Phase III. Thus, the erosive capacity of the EurIS seems to have been highest between 1.5 Ma and 0.8 Ma.
- Between 2.7 Ma and 0.8 Ma the sediment discharge to the marine margin of the EurIS was highest in the KBSIS region. During this time span the KBSIS discharged 353 $\times$ 10^6 tons/yr (2.7–1.5 Ma) and 995 $\times$ 10^6 tons/yr (1.5–0.8 Ma) of sediments onto the continental slope, building the TMF systems along the Svalbard-Western Barents Sea margin. After 0.8 Ma the sediment discharge was highest, 486 $\times$ 10^6 tons/yr, along the marine margin of the FIS.
- Based on our data, and evidence from previous studies, it is suggested that shelf edge glaciations occurred along the entire marine margin of both the KBSIS and the FIS in each of the three NHG Phases. NHG Phase I is characterized by large-scale ice sheet development with strong erosion and ice stream activity on Svalbard, while more restricted ice sheets and moderate ice stream activity occurred in other parts of the KBSIS and the FIS/BIIS although periodic shelf edge glaciations are proposed. Recurrent large-scale shelf edge glaciations with strong ice stream activity are suggested for the entire EurIS during NHG Phase II. A similar setting characterizes the EurIS during NHG Phase III, where large scale glaciations with ice streaming is suggested.
- The submergence of the Barents Sea during NHG Phase II, with its impact on the configuration of ocean currents and moisture supply, are suggested to be a key factor in explaining the significant changes in sediment distribution observed from NHG Phase II to NHG Phase III. This geographic change might be an important factor in the initiation of the MPT. It is, furthermore, also expected to have significant implications for Pliocene climate modelling.

Author contributions

This study was initiated by Hjelstuen, Sejrup and Lien. Lien compiled the data and wrote the first draft of the manuscript, except for parts of Section 6. The first draft of Section 6 was written by Zhang and Lien. All authors commented on various versions of the manuscript. Lien prepared all figures with input from all authors. All authors have approved the manuscript and agreed to its publication.

Declaration of competing interest

The authors declare that they have no known competing financial interests or personal relationships that could have appeared to influence the work reported in this paper.

Acknowledgements

The University of Bergen is acknowledged for funding of this study. Aleksandr Montelli (University of Cambridge) and Amando Lasabuda (UiT The Arctic University of Norway) are kindly thanked for providing shapefiles. We thank the Norwegian Petroleum Directorate – DISKOS Database for seismic data and Schlumberger is acknowledged for the use of the Petrel software. XZ is funded by National Science Foundation of China (no. 42075047,41988101). We acknowledge the valuable and constructive comments from three anonymous reviewers.

Appendix A. Supplementary data

Supplementary data to this article can be found online at https://doi.org/10.1016/j.quascirev.2022.107433.

References

Alexandropoulou, N., Winsborrow, M., Andreassen, K., Plaza-Faverola, A., Dessandier, P.-A., Mattingsdal, R., Baeten, N., Knies, J., 2021. A continuous seismostratigraphic framework for the western svalbard-Barents Sea margin over the last 2.7 Ma: implications for the late cenozoic glacial history of the svalbard-Barents Sea ice sheet: front. Earth Sci. 9, 656732. https://doi.org/10.3389/feart.2021.656732.

Andersen, J.L., Egholm, D.L., Knudsen, M.F., Linge, H., Jansen, J.D., Pedersen, V.K., Nielsen, S.B., Tikhomirov, D., Olsen, J., Fabel, D., Xu, S., 2018. Widespread erosion on high plateaus during recent glaciations in Scandinavia. Nat. Commun. 9. https://doi.org/10.1038/s41467-018-03280-2. Article no. 830.

Andreassen, K., Nilssen, L.C., Rafaelsen, B., Kuilman, L., 2004. Three-dimensional seismic data from the Barents Sea margin reveal evidence of past ice streams and their dynamics. Geology 32, 729–732. https://doi.org/10.1130/G20497.1.

Andreassen, K., Ødegaard, C.M., Rafaelsen, B., 2007. Imprints of Former Ice Streams, Imaged and Interpreted Using Industry Three-Dimensional Seismic Data from the South-Western Barents Sea, vol. 277. Geological Society, London, Special Publications, pp. 151–169. https://doi.org/10.1144/GSL.SP.2007.277.01.09.

Anell, I., Thybo, H., Stratford, W., 2010. Relating Cenozoic North Sea sediments to topography in southern Norway: the interplay between tectonics and climate. Earth Planet Sci. Lett. 300, 19–32. https://doi.org/10.1016/j.epsl.2010.09.009.

Anell, I., Thybo, H., Rasmussen, E., 2012. A synthesis of cenozoic sedimentation in the north sea. Basin Res. 24, 154–179. https://doi.org/10.1111/j.1365-2117.2011.00517.x.

Barker, S., Zhang, X., Jonkers, L., Lordsmith, S., Conn, S., Knorr, G., 2021. Strengthening Atlantic Inflow across the Mid-pleistocene Transition: Paleoceanography and Paleoclimatology, vol. 35, e2020PA004200. https://doi.org/10.1029/2020PA004200.

Batchelor, C.L., Ottesen, D., Dowdeswell, J.A., 2017. Quaternary evolution of the northern North Sea margin through glacigenic debris-flow and contourite deposition. J. Quat. Sci. 32, 416–426. https://doi.org/10.1002/jqs.2934.

Batchelor, C.L., Margold, M., Krapp, M., Murton, D.K., Dalton, A.S., Gibbard, P.L., Stokes, C.R., Murton, J.B., Manica, A., 2019. The configuration of Northern Hemisphere ice sheets through the Quaternary. Nat. Commun. 10, 3713. https://doi.org/10.1038/s41467-019-11601-2.

Becker, L.W.M., Sejrup, H.P., Hjelstuen, B.O., Haflidason, H., Dokken, T.M., 2018. Ocean-ice sheet interaction along the SE Nordic Seas margin from 35 to 15 ka BP. Mar. Geol. 402, 99–117. https://doi.org/10.1016/j.margeo.2017.09.003.
Bellwald, B., Planke, S., Lebedeva-Ivanova, N., Piasecka, E.D., Andreassen, K., 2019. High-resolution landform assemblage along a buried glacio-erosive surface in the SW Barents Sea revealed by P-Cable 3D seismic data. Geomorphology 332, 33–50. https://doi.org/10.1016/j.geomorph.2019.01.019.
Bellwald, B., Planke, S., Becker, L.W.M., Myklebust, R., 2020. Meltwater sediment transport as the dominating process in mid-latitude trough mouth fan formation. Nat. Commun. 11, 4645. https://doi.org/10.1038/s41467-020-18337-4.
Berends, C.J., Köhler, P., Lourens, L.J., van de Wal, R.S.W., 2021. On the cause of the mid-pleistocene transition. Rev. Geophys. 59, e2020RG000727. https://doi.org/10.1029/2020RG000727.
Broecker, W.S., Peteet, D.M., Rind, D., 1985. Does the ocean - atmosphere system have more than one stable mode of operation? Nature 315, 21–26. https://doi.org/10.1038/315021a0.
Bryn, P., Berg, K., Forsberg, C.F., Solheim, A., Kvalstad, T.J., 2005. Explaining the storegga slide. Mar. Petrol. Geol. 22, 11–19. https://doi.org/10.1016/j.marpetgeo.2004.12.003.
Buckley, F.A., 2017. A glaciogenic sequence from the early Pleistocene of the central North sea. J. Quat. Sci. 32, 145–168. https://doi.org/10.1002/jqs.2867.
Butt, F.A., Elverhøi, A., Solheim, A., Forsberg, C.F., 2000. Deciphering late cenozoic development of the western svalbard margin from ODP site 986 results. Mar. Geol. 169, 373–390. https://doi.org/10.1016/S0025-3227(00)00088-8.
Butt, F.A., Drange, H., Elverhøi, A., Otterå, O.H., Solheim, A., 2002. Modelling Late Cenozoic isostatic elevation changes in the Barents Sea and their implications for oceanic and climatic regimes: preliminary results. Quat. Sci. Rev. 21, 1643–1660. https://doi.org/10.1016/S0277-3791(02)00018-5.
Chalk, T.B., Hain, M.P., Foster, G.L., Rohling, E.J., Sexton, P.F., Badger, M.P.S., Cherry, S.G., Hasenfratz, A.P., Haug, G.H., Jaccard, S.L., Martínez-García, Pälike, H., Pancost, R.D., Wilson, P.A., 2017. Causes of ice age intensification across the Mid-Pleistocene Transition. Proc. Natl. Acad. Sci. Unit. States Am. 114, 13114–13119. https://doi.org/10.1073/pnas.1702143114.
Clark, P.U., Pollard, D., 1998. Origin of the middle Pleistocene transition by ice sheet erosion of regolith. Paleoceanogr. Paleoclimatol. 13 (1), 1–9. https://doi.org/10.1029/97PA02660.
Clark, P., Pisias, N.G., Stocker, T.F., Weaver, A.J., 2002. The role of the thermohaline circulation in abrupt climate change. Nature 415, 863–869. https://doi.org/10.1038/415863a.
Dahlgren, K.I.T., Vorren, T.O., Laberg, J.S., 2002. Late Quaternary glacial development of the mid-Norwegian margin – 65° to 68° N. Mar. Petrol. Geol. 19, 1089–1113. https://doi.org/10.1016/S0264-8172(03)00004-7.
Dahlgren, K.I.T., Vorren, T.O., Stoker, M.S., Nielsen, T., Nygård, A., Sejrup, H.P., 2005. Late Cenozoic prograding wedges on the NW European continental margin: their formation and relationship to tectonics and climate. Mar. Petrol. Geol. 22, 1089–1110. https://doi.org/10.1016/j.marpetgeo.2004.12.008.
Dowdeswell, J.A., Siegert, M.J., 1999. Ice-sheet numerical modelling and marine geophysical measurements of glacier-derived sedimentation on the Eurasian Arctic continental margins. GSA Bull. 111 (7), 1080–1097. https://doi.org/10.1130/0016-7606(1999)111<1080:ISNMAM>2.3.CO;2.
Dowdeswell, J.A., Ottesen, D., Rise, L., 2010. Rates of sediment delivery from the Fennoscandian Ice Sheet trough an ice age. Geology 38, 3–6. https://doi.org/10.1130/G25523.1.
Dowdeswell, J.A., Ottesen, D., 2013. Buried iceberg ploughmarks in the early Quaternary sediments of the central North Sea: a two-million year record of glacial influence from 3D seismic data. Mar. Geol. 344, 1–9. https://doi.org/10.1016/j.margeo.2013.06.019.
Dowsett, H., Foley, K., Stoll, D., et al., 2013. Sea Surface Temperature of the Mid-piacenzian Ocean: A Data-Model Comparison: Science Reports, vol. 3. https://doi.org/10.1038/srep02013.
Eidvin, T., Jansen, E., Rundberg, Y., Brekke, H., Grogan, P., 2000. The upper Cainozoic of the Norwegian continental shelf correlated with the deep sea record of the Norwegian Sea and the North Atlantic. Mar. Petrol. Geol. 17, 579–600. https://doi.org/10.1016/S0264-8172(00)00008-8.
Eidvin, T., Rundberg, Y., 2001. Late cainozoic stratigraphy of the tampen area (snorre and visund fields) in the northern North sea, with emphasis on the chronology of early Neogene sands. Norw. J. Geol. 81, 119–160.
Elverhøi, A., Dowdeswell, J.A., Funder, S., Mangerud, J., Stein, R., 1998a. Glacial and oceanic history of the polar north Atlantic margins: an overview. Quat. Sci. Rev. 17, 1–10. https://doi.org/10.1016/S0277-3791(97)00073-5.
Elverhøi, A., Hooke, R.LeB., Solheim, A., 1998b. Late Cenozoic erosion and sediment yield from the Svalbard-Barents Sea region: implications for understanding erosion of glacierized basins. Quat. Sci. Rev. 17, 209–241. https://doi.org/10.1016/S0277-3791(97)00070-X.
Evans, D., Harrison, Z., Shannon, P.M., Laberg, J.S., Nielsen, T., Ayers, S., Holmes, R., Hoult, R.J., Lindberg, B., Haflidason, H., Long, D., Kuijpers, A., Andersen, E.S., Bryn, P., 2005. Palaeoslides and other mass failures of Pliocene to Pleistocene age along the Atlantic continental margin of NW Europe. Mar. Petrol. Geol. 22, 1131–1148. https://doi.org/10.1016/j.marpetgeo.2005.01.010.
Faleide, J.I., Solheim, A., Fiedler, A., Hjelstuen, B.O., Andersen, E.S., Vanneste, K., 1996. Late Cenozoic evolution of the western Barents Sea-Svalbard continental margin. Global Planet. Change 12, 53–74. https://doi.org/10.1016/0921-8181(95)00012-7.
Fiedler, A., Faleide, J.I., 1996. Cenozoic sedimentation along the southwestern Barents Sea margin in relation to uplift and erosion of the shelf. Global Planet. Change 12, 75–93. https://doi.org/10.1016/0921-8181(95)00013-5.
Fjeldskaar, W., Amantov, A., 2018. Effects of glaciations on sedimentary basins. J. Geodyn. 118, 66–81. https://doi.org/10.1016/j.jog.2017.10.005.
Fransner, O., Noormets, R., Chauhan, T., Jakobsson, 2018a. Late Weichselian ice stream configuration and dynamics in Albertini Trough, northern Svalbard margin. Arktos 4, 1–22. https://doi.org/10.1007/s41063-017-0035-6.
Fransner, O., Noormets, R., Flink, A.E., Hogan, K.A., Dowdeswell, J.A., 2018b. Sedimentary processes on the continental slope off Kvitøya and Albertini troughs north of Nordaustlandet, Svalbard – the importance of structural-geological setting in trough-mouth fan development. Mar. Geol. 402, 194–208. https://doi.org/10.1016/j.margeo.2017.10.008.
Fronval, T., Jansen, E., 1996. Rapid changes in ocean circulation and heat flux in the Nordic seas during the last interglacial period. Nature 383, 806–810. https://doi.org/10.1038/383806a0.
Geissler, W.H., Jokat, W., 2004. A geophysical study of the northern Svalbard continental margin. Geophys. J. Int. 158, 50–66. https://doi.org/10.1111/j.1365-246X.2004.02315.x.
Ghil, M., Mullhaupt, A., Pestiaux, P., 1987. Deep water formation and Quaternary glaciations. Clim. Dynam. 2, 1–10.
Gibbard, P.L., Head, M.J., Walker, M.J.C., and the Subcommission on Quaternary Stratigraphy, 2010. Formal ratification of the quaternary system/period and the Pleistocene series/Epoch with a base at 2.58 Ma. J. Quat. Sci. 25, 96–102. https://doi.org/10.1002/jqs.1338.
Gibbard, P.L., Cohen, K.M., 2015. Quaternary evolution of the north Sea and the English channel. Proceed. OUGS 1, 63–74.
Gordeev, V.V., 2006. Fluvial sediment flux to the Arctic Ocean. Geomorphology 80, 94–104. https://doi.org/10.1016/j.geomorph.2005.09.008.
Haflidason, H., Aarseth, I., Haugen, J.-E., Sejrup, H.P., Løvlie, R., Reither, E., 1991. Quaternary stratigraphy of the Draugen area. Mid-Norwegian Shelf: Mar. Geol. 101, 125–146. https://doi.org/10.1016/0025-3227(91)90067-E.
Haflidason, H., King, E.L., Sejrup, H.P., 1998. Late weichselian and holocene sediment fluxes of the northern North Sea margin. Mar. Geol. 152, 189–215. https://doi.org/10.1016/S0025-3227(98)00071-1.
Haflidason, H., Lien, R., Sejrup, H.P., Forsberg, C.F., Bryn, P., 2005. The dating and morphometry of the Storegga Slide. Mar. Petrol. Geol. 22, 123–136. https://doi.org/10.1016/j.marpetgeo.2004.10.008.
Hansen, B., Østerhus, S., 2000. North Atlantic-nordic seas Exchanges. Prog. Oceanogr. 45, 109–208. https://doi.org/10.1016/S0079-6611(99)00052-X.
Harishidayat, D., Johansen, S.E., Batchelor, C., Omosanya, K.O., Ottaviani, L., 2020. Pliocene-Pleistocene glacimarine shelf to slope processes in the south-western Barents Sea. Basin Res. 33, 1315–1336. https://doi.org/10.1111/bre.12516.
Haywood, A.M., Dowsett, H.J., Dolan, A.M., 2016a. Integrating geological archives and climate models for the mid-Pliocene warm period. Nat. Commun. 7, 10646. https://doi.org/10.1038/ncomms10646.
Haywood, A.M., Dowsett, H.J., Dolan, A.M., Rowley, D., Abe-Ouchi, A., Otto-Bliesner, B., Chandler, M.A., Hunter, S.J., Lunt, D.J., Pound, M., Salzmann, U., 2016b. The Pliocene model Intercomparison project (PlioMIP) phase 2: scientific objectives and experimental design. Clim. Past 12, 663–675. https://doi.org/10.5194/cp-12-663-2016.
Henrich, R., Baumann, K.H., 1994. Evolution of the Norwegian current and the Scandinavian Ice Sheets during the past 2.6 m.y.: evidence from ODP Leg 104 biogenic carbonate and terrigenous records. Palaeogeogr. Palaeoclimatol. Palaeoecol. 108, 75–94. https://doi.org/10.1016/0031-0182(94)90023-X.
Hill, D.J., 2015. The non-analogue nature of Pliocene temperature gradients. Earth Planet Sci. Lett. 425, 232–241. https://doi.org/10.1016/j.epsl.2015.05.044.
Hjelstuen, B.O., Elverhøi, A., Faleide, J.I., 1996. Cenozoic erosion and sediment yield in the drainage area of the Storfjorden Fan. Global Planet. Change 12, 95–117. https://doi.org/10.1016/0921-8181(95)00014-3.
Hjelstuen, B.O., Sejrup, H.P., Haflidason, H., Nygård, A., Berstad, I.M., Knorr, G., 2004. Late Quaternary seismic stratigraphy and geological development of the south Vøring margin, Norwegian Sea. Quat. Sci. Rev. 23, 1847–1865. https://doi.org/10.1016/j.quascirev.2004.03.005.
Hjelstuen, B.O., Sejrup, H.P., Haflidason, H., Nygård, A., Ceramicola, S., Bryn, P., 2005. Late Cenozoic Glacial History and Evolution of the Storegga Slide Area and Adjacent Slide Flank Regions, Norwegian Continental Margin: Ormen Lange-An Integrated Study for Safe Field Development in the Storegga Submarine Area, pp. 57–69. https://doi.org/10.1016/B978-0-08-044694-3.50009-3.
Hjelstuen, B.O., Eldholm, O., Faleide, J.I., 2007. Recurrent Pleistocene mega-failures on the SW Barents Sea margin. Earth Planet Sci. Lett. 258, 605–618. https://doi.org/10.1016/j.epsl.2007.04.025.
Hjelstuen, B.O., Andreassen, E.V., 2015. North Atlantic Ocean deep-water processes and depositional environments: a study of the Cenozoic Norway Basin. Mar. Petrol. Geol. 59, 429–441. https://doi.org/10.1016/j.marpetgeo.2014.09.011.
Hjelstuen, B.O., Nygård, A., Sejrup, H.P., Haflidason, H., 2012. Quaternary denudation of southern Fennoscandia – evidence from the marine realm. Boreas 41, 379–390.
Hjelstuen, B.O., Sejrup, H.P., 2021. Latitudinal variability in the Quaternary development of the Eurasian ice sheets – evidence from the marine realm. Geology 49. https://doi.org/10.1130/G48106.1.
Hodell, D.A., Channel, J.E.T., 2016. Mode transitions in Northern Hemisphere glaciation: co-evolution of millennial and orbital variability in Quaternary climate. Clim. Past 12, 1805–1828. https://doi.org/10.5194/cp-12-1805-2016.
Hooke, R.L., 1977. Basal temperatures in polar ice sheets: a qualitative review. Quat. Res. 7, 1–13. https://doi.org/10.1016/0033-5894(77)90011-4.
Hughes, A.L.C., Clark, C.D., Jordan, C.J., 2014. Flow-pattern evolution of the last

British ice sheet. Quat. Sci. Rev. 89, 148–168. https://doi.org/10.1016/j.quascirev.2014.02.002.
Hughes, P.D., Gibbard, P.L., 2018. Global glacier dynamics during 100 ka Pleistocene glacial cycles. Quat. Res. 90 (1), 222–243. https://doi.org/10.1017/qua.2018.37.
Huuse, M., 2002. Late Cenozoic palaeogeography of the eastern North Sea Basin: climatic vs tectonic forcing of basin margin uplift and deltaic progradation. Bull. Geol. Soc. Den. 49, 145–170. https://doi.org/10.37570/bgsd-2003-49-12.
Jansen, E., Sjøholm, J., 1991. Reconstruction of glaciation over the past 6 Myr from ice-borne deposits in the Norwegian Sea. Nature 349, 600–603. https://doi.org/10.1038/349600a0.
Jansen, E., Fronval, T., Rack, F., Channel, J.E.T., 2000. Pliocene-Pleistocene ice rafting history and cyclicity in the Nordic Seas during the last 3.5 Myr. Paleoceanography 15, 709–721. https://doi.org/10.1029/1999PA000435.
King, E.L., Sejrup, H.P., Haflidason, H., Elverhøi, A., Aarseth, I., 1996. Quaternary seismic stratigraphy of the North Sea Fan: glacially-fed gravity flow aprons, hemipelagic sediments and large submarine slides. Mar. Geol. 130, 295–315. https://doi.org/10.1016/0025-3227(95)00168-9.
King, E.L., Haflidason, H., Sejrup, H.P., Løvlie, B., 1998. Glacigenic debris flows on the north sea trough mouth fan during ice stream maxima. Mar. Geol. 152, 217–246. https://doi.org/10.1016/S0025-3227(98)00072-3.
Kleiven, H.F., Jansen, E., Fronval, T., Smith, T.M., 2002. Intensification of Northern Hemisphere glaciations in the circum Atlantic region (3.5-2.4 Ma) – ice-rafted detritus evidence. Palaeogeogr. Palaeoclimatol. Palaeoecol. 184, 213–223. https://doi.org/10.1016/S0031-0182(01)00407-2.
Kleman, J., Hättestrand, C., 1999. Frozen-bed fennoscandian and Laurentide ice sheets during the last glacial maximum. Nature 402, 63–66. https://doi.org/10.1038/47005.
Kleman, J., Stroeven, A.P., Lundquist, J., 2008. Patterns of Quaternary ice sheet erosion and deposition in Fennoscandia and a theoretical framework for explanation. Geomorphology 97, 73–90. https://doi.org/10.1016/j.geomorph.2007.02.049.
Knies, J., Matthiessen, J., Vogt, C., Laberg, J.S., Hjelstuen, B.O., Smelror, M., Larsen, E., Andreassen, K., Eidvin, T., Vorren, T.O., 2009. The Plio-Pleistocene glaciation of the Barents Sea-Svalbard region: a new model based on revised Chronostratigraphy. Quat. Sci. Rev. 28, 812–829. https://doi.org/10.1016/j.quascirev.2008.12.002.
Knies, J., Mattingsdal, R., Fabian, K., Grøsfjeld, K., Baranwal, S., Husum, K., De Schepper, S., Vogt, C., Andersen, N., Matthiessen, J., Andreassen, K., Jokat, W., Nam, S.-I., Gaina, C., 2014. Effect of early Pliocene uplift on late Pliocene cooling in the Artic-Atlantic gateway. Earth Planet Sci. Lett. 387, 132–144. https://doi.org/10.1016/j.epsl.2013.11.007.
Kuhlmann, G., Langereis, C., Munsterman, D., van Leeuwen, R.J., Verreussel, R., Meulenkamp, J., Wong, T., 2006. Chronostratigraphy of late Neogene sediments in the southern North Sea Basin and paleoenvironmental interpretations. Palaeogeogr. Palaeoclimatol. Palaeoecol. 239, 426–455. https://doi.org/10.1016/j.palaeo.2006.02.004.
Laberg, J.S., Eilertsen, R.S., Vorren, T.O., 2009. The paleo-ice stream in Vestfjorden, north Norway, over the last 35 k.y.: glacial erosion and sediment yield. GSA Bull. 121 (3–4), 434–447. https://doi.org/10.1130/B26277.1.
Laberg, J.S., Andreassen, K., Knies, J., Vorren, T.O., Winsborrow, M., 2010. Late pliocene-pleistocene development of the Barents Sea ice sheet. Geology 38, 107–110. https://doi.org/10.1130/G30193.1.
Laberg, J.S., Andreassen, K., Vorren, T.O., 2012. Late Cenozoic erosion of the high-latitude southwestern Barents Sea shelf revisited. GSA Bull. 124, 77–88. https://doi.org/10.1130/B30340.1.
Laberg, J.S., Eilertsen, R.S., Salomonsen, G.R., 2018. Deglacial dynamics of the Vestfjorden – trænadjupet palaeo-ice stream, northern Norway. Boreas 47, 225–237. https://doi.org/10.1111/bor.12261.
Laberg, J.S., Stoker, M.S., Dahlgren, K.I.T., de Haas, H., Haflidason, H., Hjelstuen, B.O., Nielsen, T, Shannon, P.M., Vorren, T.O., van Weering, T.C.E., Ceramicola, S., 2005. Cenozoic alongslope processes and sedimentation on the NW European Atlantic margin. Mar. Petrol. Geol. 22, 1069–1088. https://doi.org/10.1016/j.marpetgeo.2005.01.008.
Larsen, E., Kjær, K.H., Demidov, I.N., Funder, S., Grøsfjeld, K., Houmark-Nielsen, M., Linge, H., Lysså, A., 2006. Late Pleistocene glacial and lake history of northwestern Russia. Boreas 35, 394–424. https://doi.org/10.1080/03009480600781958.
Lasabuda, A., Geissler, W.H., Laberg, J.S., Knutsen, S.-M., Rydningen, T.A., Berglar, K., 2018. Late cenozoic erosion estimates for the northern Barents Sea: quantifying glacial sediment input to the Arctic Ocean. Geochem. Geophys. Geosyst. 19, 4876–4903. https://doi.org/10.1029/2018GC007882.
Lasabuda, A.P.E., Johansen, N.S., Laberg, J.S., Faleide, J.I., Senger, K., Rydningen, T.A., Patton, H., Knutsen, S.-M., Hanssen, A., 2021. Cenozoic uplift and erosion of the Norwegian Barents Shelf – a review. Earth Sci. Rev. 217. https://doi.org/10.1016/j.earscirev.2021.103609.
Lear, C.H., Billups, K., Rickaby, R.E.M., Diester-Haass, L., Mawbey, E.M., Sosdian, S.M., 2016. Breathing more deeply: deep ocean carbon storage during the mid-Pleistocene climate transition. Geology 44, 1035–1038. https://doi.org/10.1130/G38636.1.
Lee, J.R., Busschers, F.S., Sejrup, H.P., 2012. Pre-Weichselian Quaternary glaciations of the British Isles, The Netherlands, Norway and adjacent marine areas south of 68°N: implications for long-term ice sheet development in northern Europe. Quat. Sci. Rev. 44, 213–228. https://doi.org/10.1016/j.quascirev.2010.02.027.
Lekens, W.A.H., Sejrup, H.P., Haflidason, H., Petersen, G.Ø., Hjelstuen, B.O., Knorr, G., 2005. Laminated sediments preceding heinrich event 1 in the northern North Sea and southern Norwegian sea: origin, processes and regional linkage. Mar. Geol. 216, 27–50. https://doi.org/10.1016/j.margeo.2004.12.007.
Lisiecki, L.E., Raymo, M.E., 2005. A Pliocene-Pleistocene Stack of 57 Globally Distributed $\delta^{18}O$ Records: Paleoceanography, vol. 20. https://doi.org/10.1029/2004PA001071. PA 1003.
Løseth, H., Dowdeswell, J.A., Batchelor, C.L., Ottesen, D., 2020. 3D sedimentary architecture showing the inception of an Ice Age. Nat. Commun. 11, 2975. https://doi.org/10.1038/s41467-020-16776-7.
Mattingsdal, R., Knies, J., Andreassen, K., Fabian, K., Husum, K., Grøsfjeld, K., De Schepper, S., 2014. A new 6 Myr stratigraphic framework for the Atlantic-Arctic Gateway. Quat. Sci. Rev. 92, 170–178. https://doi.org/10.1016/j.quascirev.2013.08.022.
Millimann, J.D., Syvitski, J.P.M., 1992. Geomorphic/Tectonic control of sediment discharge to the ocean: the importance of small mountainous rivers. J. Geol. 100, 525–544. https://doi.org/10.1086/629606.
Montelli, A., Dowdeswell, J.A., Ottesen, D., Johansen, S.E., 2017. Ice-sheet dynamics through the Quaternary on the mid-Norwegian continental margin inferred from 3D seismic data. Mar. Petrol. Geol. 80, 228–242. https://doi.org/10.1016/j.marpetgeo.2016.12.002.
Montelli, A., Dowdeswell, J.A., Ottesen, D., Johansen, S.E., 2018a. Architecture and sedimentary processes on the mid-Norwegian continental slope: a 2.7 Myr record from extensive seismic evidence. Quat. Sci. Rev. 192, 185–207. https://doi.org/10.1016/j.quascirev.2018.05.034.
Montelli, A., Dowdeswell, J.A., Ottesen, D., Johansen, S.E., 2018b. 3D seismic evidence of buried iceberg ploughmarks from the mid-Norwegian continental margin reveals largely persistent North Atlantic Current through the Quaternary. Mar. Geol. 399, 66–83. https://doi.org/10.1016/j.margeo.2017.11.016.
Mudelsee, M., Schulz, M., 1997. The Mid-Pleistocene climate transition: onset of 100 ka cycle lags ice volume build-up by 280 ka. Earth Planet Sci. Lett. 151, 117–123. https://doi.org/10.1016/S0012-821X(97)00114-3.
Newton, A.M.W., Huuse, M., Brocklehurst, S.H., 2018. A persistent Norwegian Atlantic current through the Pleistocene glacials. Geophys. Res. Lett. 45, 5599–5608. https://doi.org/10.1029/2018GL077819.
Nielsen, T., De Santis, L., Dahlgren, K.I.T., Kuijpers, A., Laberg, J.S., Nygård, A., Praeg, D., Stoker, M.S., 2005. A comparison of the NW European glaciated margin with other glaciated margins. Mar. Petrol. Geol. 22, 1149–1183. https://doi.org/10.1016/j.marpetgeo.2004.12.007.
Nielsen, T., Rasmussen, T.L., Ceramicola, S., Kuijpers, A., 2007. Quaternary sedimentation, margin architecture and ocean circulation variability around the Faroe Islands, North Atlantic. Quat. Sci. Rev. 26, 1016–1036. https://doi.org/10.1016/j.quascirev.2006.12.005.
Nygård, A., Sejrup, H.P., Haflidason, H., Bryn, P., 2005. The glacial North Sea Fan, southern Norwegian Margin: architecture and evolution from the upper continental slope to the deep-sea basin. Mar. Petrol. Geol. 22, 71–84. https://doi.org/10.1016/j.marpetgeo.2004.12.001.
Nygård, A., Sejrup, H.P., Haflidason, H., Lekens, W.A.H., Clark, C.D., Bigg, G.R., 2007. Extreme sediment and ice discharge from marine-based ice streams: new evidence from the North Sea. Geology 35 (5), 395–398. https://doi.org/10.1130/G23364A.1.
Orvik, K.A., Niiler, P., 2002. Major pathways of Atlantic water in the northern North Atlantic and Nordic seas toward Arctic. Geophys. Res. Lett. 29, 2. https://doi.org/10.1029/2002GL015002.
Ottesen, D., Dowdeswell, J.A., Rise, L., 2005. Submarine landforms and the reconstruction of fast-flowing ice streams within a large Quaternary ice sheet: the 2500-km-long Norwegian-Svalbard margin (57°-80°N). GSA Bull. 117 (7–8), 1033–1050. https://doi.org/10.1130/B25577.1.
Ottesen, D., Rise, L., Andersen, E.S., Bugge, T., Eidvin, T., 2009. Geological evolution of the Norwegian continental shelf between 61°N and 68°N during the last 3 million years. Norw. J. Geol. 89, 251–265.
Ottesen, D., Dowdeswell, J.A., Bugge, T., 2014. Morphology, sedimentary infill and depositional environments of the early quaternary North Sea basin (52°-62°N). Mar. Petrol. Geol. 56, 123–146. https://doi.org/10.1016/j.marpetgeo.2014.04.007.
Ottesen, D., Batchelor, C.L., Dowdeswell, J.A., Løseth, H., 2018. Morphology and pattern of quaternary sedimentation in the north Sea Basin (52°-62°N). Mar. Petrol. Geol. 98, 836–859. https://doi.org/10.1016/j.marpetgeo.2018.08.022.
Owen, M.J., Long, D., 2016. Barra Fan: a Major Glacial Depocentre on the Western Continental Margin of the British Isles, vol. 46. Geological Society, London, Memoirs, pp. 359–360. https://doi.org/10.1144/M46.76.
Patruno, S., Scisciani, V., Helland-Hansen, W., D'Intino, N., Reid, W., Pellegrini, C., 2019. Upslope-climbing shelf-edge clinoforms and the stepwise evolution of the northern European glaciation (lower Pleistocene Eridanos Delta system, U.K. North Sea): when sediment supply overwhelms accommodation. Basin Res. 32, 224–239. https://doi.org/10.1111/bre.12379.
Patton, H., Hubbard, A., Andreassen, K., Winsborrow, M., Stroeven, A.P., 2016. The build-up, configuration, and dynamical sensitivity of the Eurasian ice-sheet complex to late Weichselian climatic and oceanic forcing. Quat. Sci. Rev. 153, 97–121. https://doi.org/10.1016/j.quascirev.2016.10.009.
Patton, H., Hubbard, A., Andreassen, K., Auriac, A., Whitehouse, P.L., Stroeven, A.P., Shackleton, C., Winsborrow, M., Heyman, J., Hall, A.M., 2017. Deglaciation of the Eurasian ice sheet complex. Quat. Sci. Rev. 169, 148–172. https://doi.org/10.1016/j.quascirev.2017.05.019.
Pena, L.D., Goldstein, S.L., 2014. Thermohaline circulation crisis and impacts during the mid-Pleistocene transition. Science 345, 318–322. https://doi.org/10.1126/science.1249770.
Pope, E.L., Talling, P.J., Cofaigh, C.Ó., 2018. The relationship between ice sheets and

submarine mass movements in the Nordic Seas during the Quaternary. Earth Sci. Rev. 178, 208–256. https://doi.org/10.1016/j.earscirev.2018.01.007.
Rea, B.R., Newton, A.M.W., Lamb, R.M., Harding, R., Bigg, G.R., Rose, P., Spagnolo, M., Huuse, M., Cater, J.M.L., Archer, S., Buckley, F., Halliyeva, M., Huuse, J., Cornwell, D.G., Brocklehurst, S.H., Howell, J.A., 2018. Extensive marine-terminating ice sheets in Europe from 2.5 million years ago. Sci. Adv. 4, 11. https://doi.org/10.1126/sciadv.aar8327.
Rebesco, M., Hernández-Molina, F.J., Van Rooij, D., Wåhlin, A., 2014. Contourites and associated sediments controlled by deep-water circulation processes: state-of-the-art and future considerations. Mar. Geol. 352, 111–154. https://doi.org/10.1016/j.margeo.2014.03.011.
Reinardy, B.T.I., Hjelstuen, B.O., Sejrup, H.P., Augedal, H., Jørstad, A., 2017. Late Pliocene-Pleistocene environments and glacial history of the northern North Sea. Quat. Sci. Rev. 158, 107–126. https://doi.org/10.1016/j.quascirev.2016.12.022.
Rise, L., Ottesen, D., Berg, K., Lundin, E., 2005. Large-scale development of the mid-Norwegian margin during the last 3 million years. Mar. Petrol. Geol. 22, 33–44. https://doi.org/10.1016/j.marpetgeo.2004.10.010.
Rise, L., Ottesen, D., Longva, O., Solheim, A., Andersen, E.S., Ayers, S., 2006. The Sklinnadjupet slide and its relation to the Elsterian glaciation on the mid-Norwegian margin. Mar. Petrol. Geol. 23, 569–583. https://doi.org/10.1016/j.marpetgeo.2006.05.005.
Rise, L., Chand, S., Hjelstuen, B.O., Haflidason, H., Røe, R., 2010. Late Cenozoic development of the south Vøring margin, mid-Norway. Mar. Petrol. Geol. 27, 1789–1803. https://doi.org/10.1016/j.marpetgeo.2010.09.001.
Rydningen, T.A., Laberg, J.S., Kolstad, V., 2016. Late Cenozoic evolution of high-gradient trough mouth fans and canyons on the glaciated continental margin offshore Troms, northern Norway – paleoclimatic implications and sediment yield. TGSA Bull. 128, 576–596. https://doi.org/10.1130/B31302.1.
Rydningen, T.A., Høgseth, G.V., Lasabuda, A.P.E., Laberg, J.S., Safronova, M., Forwick, M., 2020. An early Neogene—early quaternary contourite drift system on the SW Barents Sea continental margin. Norwegian Arctic: Geochem. Geophys. Geosyst. 21, e2020GC009142. https://doi.org/10.1029/2020GC009142.
Sarkar, S., Berndt, C., Chabert, A., Masson, D.G., Minshull, T.A., Westbrook, G.K., 2011. Switching of a paleo-ice stream in northwest Svalbard. Quat. Sci. Rev. 30, 1710–1725. https://doi.org/10.1016/j.quascirev.2011.03.013.
Sejrup, H.P., King, E.L., Aarseth, I., Haflidason, H., Elverhøi, A., 1996. Quaternary Erosion and Depositional Processes: Western Norwegian Fjords, Norwegian Channel and North Sea Fan, vol. 117. Geological Society Special Publications, pp. 187–202. https://doi.org/10.1144/GSL.SP.1996.117.01.11.
Sejrup, H.P., Larsen, E., Landvik, J., King, E.L., Haflidason, H., Nesje, A., 2000. Quaternary glaciations in southern Fennoscandia: evidence from southwestern Norway and the northern North Sea region. Quat. Sci. Rev. 19, 667–685. https://doi.org/10.1016/S0277-3791(99)00016-5.
Sejrup, H.P., Hjelstuen, B.O., Dahlgren, K.I.T., Haflidason, H., Kuijpers, A., Nygård, A., Praeg, Stoker, M.S., Vorren, T.O., 2005. Pleistocene glacial history of the NW European continental margin. Mar. Petrol. Geol. 22, 1111–1129. https://doi.org/10.1016/j.marpetgeo.2004.09.007.
Solheim, A., Andersen, E.S., Elverhøi, A., Fiedler, A., 1996. Late Cenozoic depositional history of the western Svalbard continental shelf, controlled by subsidence and climate. Global Planet. Change 12, 135–148. https://doi.org/10.1016/0921-8181(95)00016-X.
Solheim, A., Faleide, J.I., Andersen, E.S., Elverhøi, A., Forsberg, C.F., Vanneste, K., Uenzelmann-Neben, G., Channel, J.E.T., 1998. Late Cenozoic seismic stratigraphy and glacial geological development of the east Greenland and Svalbard-Barents Sea continental margins. Quat. Sci. Rev. 17, 155–184. https://doi.org/10.1016/S0277-3791(97)00068-1.
Solheim, A., Berg, K., Forsberg, C.F., Bryn, P., 2005. The Storegga Slide complex: repetitive large scale sliding with similar cause and development. Mar. Petrol. Geol. 22, 97–107. https://doi.org/10.1016/j.marpetgeo.2004.10.013.
Steer, P., Huismans, R.S., Valla, P.G., Gac, S., Herman, F., 2012. Bimodal Plio-Quaternary glacial erosion of fjords and low relief surfaces in Scandinavia. Nat. Geosci. 5, 635–639. https://doi.org/10.1038/ngeo1549.
Stoker, M.S., Praeg, D., Hjelstuen, B.O., Laberg, J.S., Nielsen, T., Shannom, P.M., 2005. Neogene stratigraphy and the sedimentary and oceanographic development of the NW European Atlantic margin. Mar. Petrol. Geol. 22, 977–1005. https://doi.org/10.1016/j.marpetgeo.2004.11.007.
Storvoll, V., Bjørlykke, K., Mondol, N.H., 2005. Velocity-depth trends in mesozoic and cenozoic sediment from the Norwegian shelf. AAPG (Am. Assoc. Pet. Geol.) Bull. 89, 359–381. https://doi.org/10.1306/10150404033.
Svendsen, J.I., Mangerud, J., Miller, G.H., 1989. Denudation rates in the Arctic estimated from lake sediments on Spitsbergen. Svalbard: Palaeogeogr. Palaeoclimatol. Palaeoecol. 76, 153–168. https://doi.org/10.1016/0031-0182(89)90108-9.
Svendsen, J.I., Alexanderson, H., Astakhov, V.I., Demidov, I., Dowdeswell, J.A., Funder, S., Gataullin, V., Henriksen, M., Hjort, C., Houmark-Nielsen, M., Hubberten, H.W., Ingólfsson, Ó., Jakobsson, M., Kjær, K.H., Larsen, E., Lokrantz, H., Lunkka, J.P., Lyså, A., Mangerud, J., Matiouchkov, A., Murray, A., Möller, P., Niessen, F., Nikolskaya, O., Polyak, L., Saarnistro, M., Siegert, C., Siegert, M.J., Spielhagen, R.F., Stein, R., 2004. Late Quaternary ice sheet history of northern Eurasia. Quat. Sci. Rev. 23, 1229–1271. https://doi.org/10.1016/j.quascirev.2003.12.008.
Syvitski, J.P.M., 2002. Sediment discharge variability in Arctic rivers: implications for a warmer future. Polar Res. 21 (2), 323–330. https://doi.org/10.3402/polar.v21i2.6494.
Sættem, J., Poole, D.A.R., Ellingsen, L., Sejrup, H.P., 1992. Glacial geology of outer Bjørnøyrenna, southwestern Barents Sea. Mar. Geol. 103, 15–51. https://doi.org/10.1016/0025-3227(92)90007-5.
Tegzes, A.D., Jansen, E., Lorentzen, T., Telford, R.J., 2017. Northward oceanic heat transport in the main branch of the Norwegian Atlantic Current over the late Holocene. Holocene 27 (7), 1034–1044. https://doi.org/10.1177/0959683616683251.
Thierens, M., Pirlet, H., Colin, C., Latruwe, K., Vanhaecke, F., Lee, J.R., Stuut, J.-B., Titschack, J., Huvenne, V.A.I., Dorschel, B., Wheeler, A.J., Henriet, J.-P., 2012. Ice-rafting from the British-Irish ice sheet since the earliest Pleistocene (2.6 million years ago): latitudinal ice-sheet growth in the North Atlantic region. Quat. Sci. Rev. 44, 229–240. https://doi.org/10.1016/j.quascirev.2010.12.020.
Turrel, W.R., Slesser, G., Adams, R.D., Payne, R., Gillibrand, P.A., 1999. Decadal variability in the composition of Faroe Shetland Channel bottom water. Deep-Sea Res. Part 1: Oceanograph. Res. Pap. 46, 1–25. https://doi.org/10.1016/S0967-0637(98)00067-3.
Tziperman, E., Gildor, H., 2003. On the mid-Pleistocene transition to 100-kyr glacial cycles and the asymmetry between glaciation and deglaciation times. Paleoceanography 18 (1), 1001. https://doi.org/10.1029/2001pa000627.
Vanneste, M., Mienert, J., Bünz, S., 2006. The Hinlopen Slide: a giant, submarine slope failure on the northern Svalbard margin. Arctic Ocean: Earth Planet Sci. Lett. 245, 373–388. https://doi.org/10.1016/j.epsl.2006.02.045.
Van Hinte, J.E., 1978. Geohistory Analysis – Application of micropaleontology in Exploration geology. Am. Assoc. Petrol. Geol. Bull. 62 (2), 201–222.
Vorren, T.O., Richardsen, G., Knutsen, S.-M., Henriksen, E., 1991. Cenozoic erosion and sedimentation in the western Barents Sea. Mar. Petrol. Geol. 8, 317–340. https://doi.org/10.1016/0264-8172(91)90086-G.
Vorren, T.O., Laberg, J.S., 1997. Trough mouth fans – palaeoclimate and ice-sheet monitors. Quat. Sci. Rev. 16, 865–881. https://doi.org/10.1016/S0277-3791(97)00003-6.
Vorren, T.O., Laberg, J.S., Blaume, F., Dowdeswell, J.A., Kenyon, N.H., Mienert, J., Rumohr, J., Werner, F., 1998. The Norwegian-Greenland sea continental margins: morphology and late quaternary sedimentary processes and environment. Quat. Sci. Rev. 17, 273–302. https://doi.org/10.1016/S0277-3791(97)00072-3.
Waage, M., Bünz, S., Bøe, R., Mienert, J., 2018. High resolution 3D seismic exhibit new insights into the middle-late Pleistocene stratigraphic evolution and sedimentary processes of the Bear Island trough mouth fan. Mar. Geol. 403, 139–149. https://doi.org/10.1016/j.margeo.2018.05.006.
Wellner, J., Lowe, A., Shipp, S., Anderson, J., 2001. Distribution of glacial geomorphic features on the Antarctic continental shelf and correlation with substrate: implications for ice behavior. J. Glaciol. 47 (158), 397–411. https://doi.org/10.3189/172756501781832043.
Willenbring, J.K., von Blanckenburg, F., 2010. Long-term stability of global erosion rates and weathering during late-Cenozoic cooling. Nature 465, 211–214. https://doi.org/10.1038/nature09044.
Willeit, M., Ganopolski, A., Calov, R., Brovkin, V., 2019. Mid-Pleistocene transition in glacial cycles explained by declining CO_2 and regolith removal. Sci. Adv. 5. https://doi.org/10.1126/sciadv.aav7337. Article no. Eaav7337.
Yehudai, M., Kim, J., Pena, L.D., Jaume-Segui, M., Knudson, K.P., Bolge, L., Malinverno, A., Bickert, T., Goldstein, S.L., 2021. Evidence for a Northern Hemispheric trigger of the 100,000-y glacial cyclicity. Proc. Natl. Acad. Sci. Unit. States Am. 118 (46), e2020260118. https://doi.org/10.1073/pnas.2020260118.
Zhang, Z., Yan, Q., Zhang, R., Colleoni, F., Ramstein, G., Dai, G., Jakobsson, M., O'Regan, M., Liess, S., Rousseau, D.-D., Wu, N., Farmer, E.J., Contoux, C., Guo, C., Tan, N., Guo, Z., 2020. Rapid Waxing and Waning of Beringian Ice Sheet Reconcile Glacial Climate Records from Around North Pacific: Climates of the Past preprint (not published).
Zieba, K.J., Omosanya, K.O., Knies, J., 2017. A flexural isostasy model for the Pleistocene evolution of the Barents Sea bathymetry. Norw. J. Geol. 97, 1–19. https://doi.org/10.17850/njg97-1-01.